MODEL FOR AN IMMERSED, COLLECTOR SIDE HEAT EXCHANGER

by

ROBERT EDWARD MATES JR.

A thesis submitted in partial fulfillment of the

requirements for the degree of

MASTER OF SCIENCE

in MECHANICAL ENGINEERING

at the

UNIVERSITY OF WISCONSIN-MADISON

1987

MODEL FOR AN IMMERSED, COLLECTOR SIDE HEAT EXCHANGER

APPROVED

Professor William A. Beckman

William A Beckman

date 12/7/81

ACKNOWLEDGMENTS

I am very grateful to have had the opportunity to work under the guidance of Professor John W. Mitchell. I would also like to direct my gratitude towards Professors W. A. Beckman and J. A. Duffie for their contributions to this work. I am indebted to the staff and fellow graduate students of the Solar Energy Laboratory for their academic and moral support and their efforts in behalf of my sense of humor. I am also grateful for the hockey rink down the block which helped me release a lot of tension safely and effectively three times a week. Finally, I would like to thank my parents and family for their sincere support throughout the last year and a half.

Abstract

A theoretical model has been developed for the heat transfer from a tubular collector side heat exchanger immersed in a hot water tank. This is a general model for any immersed heat exchanger geometry and orientation. The Petukhov correlation was used to calculate the interior forced convection heat transfer coefficient. The exterior natural convection heat transfer coefficient was calculated using the Morgan correlation combined with a multiplicative constant M to account for any natural convection enhancement effects. The constant M can only be found through an experimental test of the heat exchanger. The model calculates UA for the heat exchanger by averaging values of UA at the inlet and exit. The model performance was compared with experimental test data for four heat exchanger designs from SERI, and an enhancement of natural convection heat transfer of 30% to 80% was found to exist among the heat exchangers. The model was integrated into a solar domestic hot water heating system and year long simulations were carried out using the TRNSYS simulation package. The value of M was found to have little effect on the yearly solar fraction for systems employing the SERI heat exchanger designs at flow rates of 0.015 l/s m^2 as there was a low collector area penalty associated with these systems.

TABLE OF CONTENTS

LIST OF FIGURES AND TABLES

List of Figures and Tables (continued)

Nomenclature

Symbols used in this thesis which do not appear below are defined locally in the text.

A_c	contact area
A_ε	effective heat exchanger exterior heat transfer area
A_f	fraction of exterior heat transfer area due to fins
A_o	total heat exchanger exterior heat transfer area
C	constant in Morgan correlation
CD	contact diameter
Cp	specific heat
e	exponential
F	solar fraction, or fraction of yearly load supplied by solar energy
f	friction factor
g	gravitational acceleration
h_c	contact heat transfer coefficient
h_i	tube interior heat transfer coefficient
h_o	tube exterior heat transfer coefficient
ID	inside tube diameter
K	Kelvin
k	thermal conductivity

Nomenclature (cont'd)

K1,K2	constants in Petukhov correlation
L	tube length
M	natural convection enhancement factor
m	constant in Morgan correlation
$\dot{m}$	mass flow rate
Nu	Nusselt number
NTU	number of heat transfer units
OD	outside tube diameter
Pr	Prandtl number
q	heat flow
R	thermal resistance
Ra_D	Rayleigh number based on exterior diameter
Re	Reynolds number
T	temperature
T_i	tube inlet temperature
T_o	tube exit temperature
T_{onew}	new tube exit temperature in iterative algorithm
T_{ref}	reference temperature
T_s	water storage or ambient temperature
T_w	tube wall temperature
T_{wnew}	new tube wall temperature in iterative algorithm

Nomenclature (cont'd)

UA	overall heat transfer coefficient-area product
UAI	heat transfer coefficient-area for the interior heat transfer coefficient and the wall resistance
U_m	mean fluid velocity inside circular duct

Greek Symbols

α	thermal diffusivity
β	coefficient of thermal expansion
ε	heat exchanger effectiveness
η	fin efficiency
μ_b	dynamic viscosity at fluid bulk temperature
μ_w	dynamic viscosity at wall temperature
ν	kinematic viscosity
π	Pi
ρ	density
σ	standard deviation

1.0 Introduction

Immersed coil heat exchangers have become important components in domestic solar heating systems. Many solar domestic hot water systems employ supply side heat exchangers, which transfer energy from the hot collector fluid loop to the storage medium. A supply side heat exchanger transfers heat through forced convection on the interior, collector fluid side of the coil. The heat is then transferred via natural convection from the exterior of the coil to the storage medium. The performance of a supply side heat exchanger can have a great impact on the performance of the entire solar energy system, as noted by Duffie and Beckman [1]. Simulations of solar systems therefore depend on the accuracy of the mathematical model of the heat exchanger and storage tank. The first purpose of this study, then, is to devise an accurate, general mathematical model for an immersed, coiled tube, supply side heat exchanger. A second goal is to make the model useful by translating it into a computationally compact program to be used in simulation software such as TRNSYS [2].

There has been a limited amount of research done concerning combined forced and natural convection from immersed heat exchangers. Two experimental studies, by Feiereisen [4] and Farrington [5], form the data base for the development of this model. Feiereisen experimentally studied four different

coil configurations. The coils examined included: (1) a horizontal, multi-pass, smooth tube coil, (2) a horizontal, spiraling, finned tube coil and (3) a horizontal, single-pass, smooth-tube coil. The fourth configuration (4) was a series combination of two type (1) coils placed one above the other. Data were presented in the form of an average Nusselt number as a function of an average Rayliegh number for the entire coil in the following form:

$$Nu = C\ Ra_D^m \qquad (1.1.1)$$

The constant m = 0.25 and the constant C is used to fit the correlation to the observed data for each heat exchanger. Heat exchanger parameters such as effectiveness and the overall loss coefficient-area product UA were also presented. Finally, stratification in the tank was found to be nonexistent except during the period of a load draw, after which the stratification again disappeared. A heat exchanger model was also proposed by Feiereisen for use in simulations. The model was an external, zero capacitance, sensible heat exchanger with constant ε, and assumes forced flow on both sides of the exchanger and a fully mixed tank.

Farrington [5] provided the bulk of the experimental backround for this study. Four heat exchanger configurations were examined: a smooth tube coil (5), a finned spiral tube (6) a finned single wall bayonet (7) and finned double wall bayonet (8). The tests were performed in an apparatus resembling a standard domestic hot water heating system. The experimental

procedure consisted of heating a storage tank with the heat exchanger situated at the bottom of the tank. The raw data from the experiments consisted of system temperatures and heat transfer calculations for each data run. These data will be presented in Chapter 3. The overall performance data, including effectiveness, heat flow and overall UA for each test were reported. Also, an average Nusselt-Rayleigh correlation for each heat exchanger at each flow rate was presented in the form used by Feiereisen (eq. 1.1.1). Finally, four thermocouples attached at various heights along the storage tank showed no stratification during heating except for a thin layer of fluid below the heat exchanger.

Three models were proposed by Farrington for the heat exchanger, two of which were analytical and one which was a finite difference model. The first analytical model was based on the assumptions of a negligible tube interior heat transfer resistance and a constant exterior heat transfer coefficient along the tube wall. The natural convective heat transfer coefficient was based on the difference between the heat exchanger inlet temperature and the bulk storage tank temperature. The effectiveness was then derived from an energy balance between the hot side fluid and the bulk storage fluid. A temperature correction factor was added to account for interior heat transfer coefficient. The second analytical model was similar to the first model except that it includes the dependence of the natural convective heat transfer coef-

ficient on the difference between the local tube temperature and the bulk tank temperature, and the exterior heat transfer coefficient varies with position on the tube. Finally, a two dimensional steady state finite difference model was proposed using four radial nodes from the centerline of the tube to the bulk tank fluid and 50 axial nodes. The interior and exterior heat transfer coefficients varied along the length of the tube. All three models assume a single horizontal tube which does not account for heat exchanger geometry.

This thesis contains the following information. Chapter 2 is a description of the model itself, and is divided into sections based on the major program subroutines describing the basic equations in. Chapter 3 is a comparison of model performance versus experimental data from Feiereisen [4] and Farrington [5]. Chapter 4 is a discussion of the performance of the model and the method used to include natural convection enhancement effects. Finally, Chapter 5 presents conclusions and recommendations for further study.

2.0 Model

The mathematical model is based on the assumption that the heat exchanger is an infinitely long tube in an infinite medium. Standard correlations are used to determine the interior and exterior heat transfer coefficients, and an energy balance from the hot side to the cold side of the tube is used to find unknown temperatures. A correction factor is used in the correlation for the exterior heat transfer coefficient which accounts for the coiled geometry of the tube and the confining walls of the storage tank.

The model will be explained in this chapter according to the structure of the program that performs the model calculations. The program itself makes use of subroutines which perform the rudimentary calculations, such as heat transfer coefficients or property values. Other subroutines perform umbrella functions, such as solving energy balance equations or controlling the calculation of steady state heat transfer. Each subroutine in the program will be examined in a separate section in this chapter. An overall flowchart, shown in figure 1, provides a schematic to aid in the explanation.

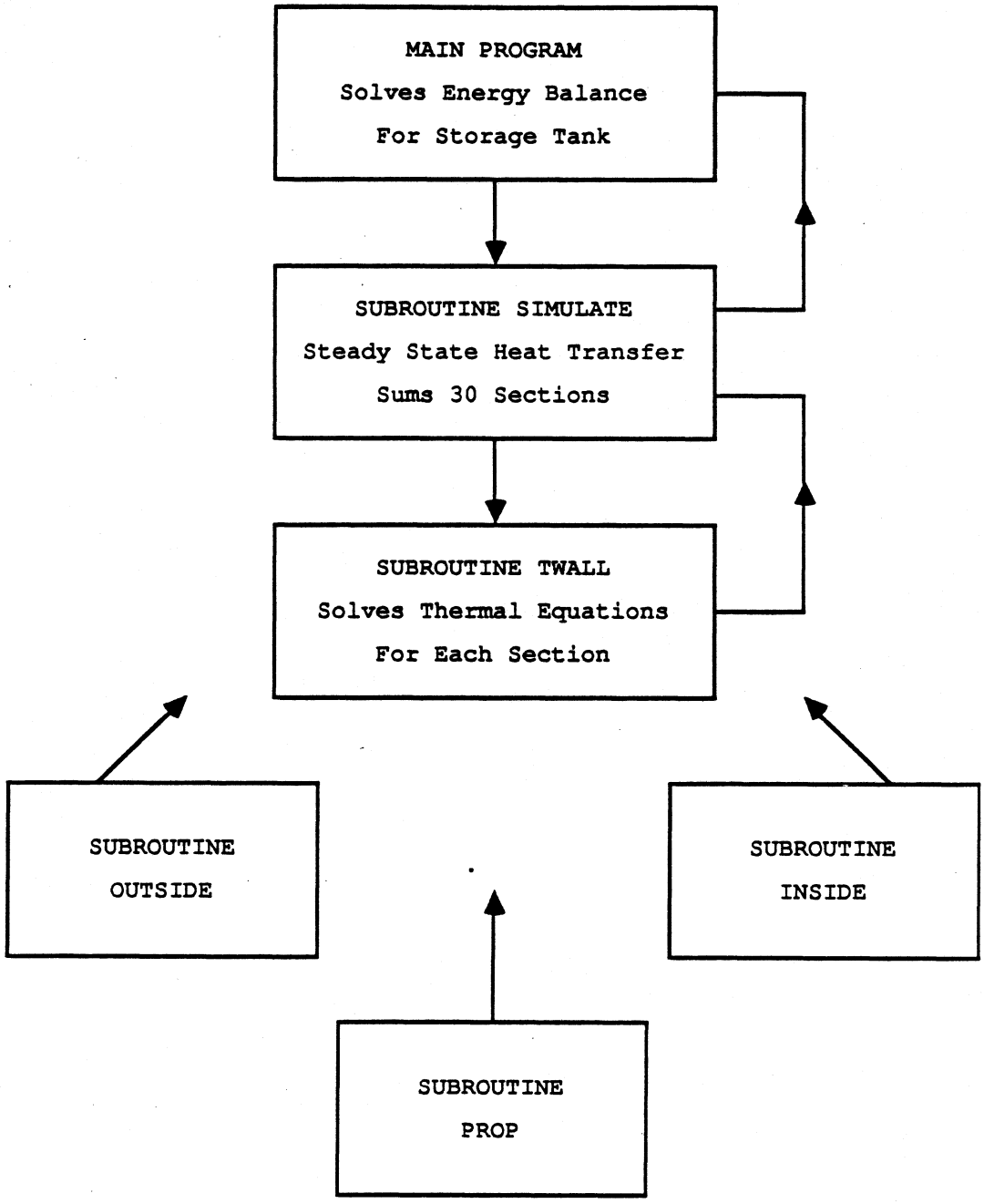

Figure 1. Benchmark Program Schematic

Three separate programs have been developed to perform the same model calculations in varying degrees of simplicity. The model equations remain essentially the same, but the method of solution is gradually simplified to reduce the CPU time associated with the simulation. Large system simulations, such as those performed by TRNSYS [2], require component subroutines which are computationally efficient.

The original or BENCHMARK program was developed to validate the model against the data of Farrington. The heat exchanger in the BENCHMARK program is divided into 30 sections along the length of the tube. The steady state heat transfer for each section is calculated given the inlet water temperature, flow rate and the storage tank temperature. The heat flows from each section are added together for a steady state heat flow from the exchanger.

A second simpler program, called SIMPLE, calculates a UA for the entire length of the tube from an average of UA values at the heat exchanger inlet and exit. The equations for heat transfer coefficients used in SIMPLE are identical to those used in BENCHMARK. SIMPLE eliminates the position dependence of the calculations. Finally, a third program calculates a constant effectiveness for the heat exchanger given some set of representative thermal conditions and uses this effectiveness to find the heat flow for each time step. The constant effectiveness program, called CONSTE, eliminates the time dependence in the calculations.

The BENCHMARK program is diagrammed in figure 1 and is the program on which the discussion of the model is based. A listing of the BENCHMARK program can be found in appendix A, the average UA program SIMPLE in appendix B, and the constant effectiveness program CONSTE is listed in appendix C. The simulation results of each program are evaluated in Chapter 3.

2.1 Assumptions

Several assumptions have been made for the model which simplify the mathematics and have been shown to be valid under experimental conditions.

The first assumption is that of a quasistatic heat transfer over discrete, short time steps. This assumption allows the calculation of a constant heat transfer over a short period of time as an approximation of the instantaneous heat transfer function.

The second assumption is that the tank is fully mixed during the heat exchange. This has been shown by both Feiereisen [4] and Farrington [5]. Feiereisen observed that his tank had a stratified condition only during a load draw, after which the tank reverted to a fully mixed condition. The fully mixed assumption also agrees with the idea that natural convective currents travel from the bottom to the top of the tank as cold water at the bottom is heated to a point where it

is the hottest water in the tank. Bouyant forces move the heated water upward mixing it with the rest of the storage medium along the way.

The stratification during a load draw is not addressed by the model for several reasons. First, as far as heat transfer from the coil is concerned, the tank is always fully mixed, because even during a load draw heat transfer from the coil will induce mixing, so a fully mixed tank is a good approximation. Second, if there is no load draw or heat transfer from the coil, the tank will not stratify on its own. Stratification may occur during times where there is a load draw with no heat transfer from the exchanger, but the effects of this stratification are assumed to be negligible.

A third assumption is that the enhancement that occurs due to the coiled geometry of the heat exchanger or the confining walls of the storage tank can be accounted for by including a multiplicative constant M in the Morgan correlation for natural convection heat transfer from an infinitely long tube in an infinite medium. The constant M is an average enhancement factor over the length of the tube.

A fourth assumption is that the copper wall of the heat exchanger tube does not offer a significant resistance to heat transfer. Heat exchangers constructed of copper tubing have negligible wall thickness (the average wall thickness for the four heat exchangers used by Farrington was about 2.5 mm). Heat exchangers with double wall construction do present si-

nificant wall resistance to heat transfer and a contact coefficient is employed to account for this resistance.

2.2 Water Properties

The subroutine PROP in the program calculates the physical properties of the working fluid given the temperature. The working fluid on both sides of the heat exchanger in the model is water, as this is the working fluid used by Farrington [5]. Other fluids, such as those which contain antifreeze for the collector loop, could be accomodated using a similar, supplementary subroutine in the program. Several properties of water vary greatly over a temperature range from freezing to boiling, most notably the Prandtl number, so for purposes of numerical accuracy the fluid property variation must be taken into account. This is important, as the UA along the length of the tube may change up to 40% due to variable water properties resulting from temperature changes on both sides of the exchanger wall. The subroutine PROP calculates property values from correlations as a function of temperature. These correlations are derived using property data and the MINPACK nonlinear regression package LMDIF1 [8]. The density values originated from Schmidt [9]. The values for the Prandtl number, thermal conductivity, kinematic viscosity and specific heat came from Incropera and Dewitt [10]. The value of β, the

coefficient of thermal expansion, used in the calculation of the Rayleigh number, was found numerically using an approximation of the definition:

$$\beta = \frac{1}{\rho} \frac{\partial \rho}{\partial T} \qquad (2.2.1)$$

and the density and temperature data. Correlations for water properties were found between the temperatures of 280 K and 370 K, temperatures near the freezing and boiling points of water. The correlations are detailed in Appendix D.

2.3 Interior Heat Transfer Coefficient

Subroutine INSIDE calculates the interior, forced convective heat transfer coefficient given the fluid mass flow rate, temperature, and inside tube diameter. The phenomenon of forced convection inside tubes has been well defined by Petukhov [6] for turbulent flow conditions. The Petukhov correlation defines an average Nusselt number over a discrete length of tube as a function of the Reynolds and Prandtl numbers:

$$\overline{Nu} = \frac{(f/8)\ Re\ Pr\ (\mu_b/\mu_w)^{0.25}}{K1+K2\,(f/8)^{1/2}(Pr^{2/3}-1)} \qquad (2.3.1)$$

where

$$f = (1.82\log_{10}Re - 1.64)^{-2} \qquad (2.3.2)$$

$$K1 = 1.0 + 3.4\ f \tag{2.3.3}$$

$$K2 = 11.7 + \frac{1.8}{Pr^{1/3}} \tag{2.3.4}$$

and

$$Re = \frac{U_m\ ID}{\nu} \tag{2.3.5}$$

The Petukhov correlation is defined for the following range of the Reynolds number

$$10^4 < Re < 5 \times 10^6$$

The average heat transfer coefficient for the length of tube being analyzed is then:

$$\overline{h_i} = \frac{k\ \overline{Nu}}{ID} \tag{2.3.6}$$

The flow conditions found at flow rates of 300 Kg/Hr and higher fall within the turbulent velocities for tube diameters used by Farrington [5]. Low flow systems are also useful, and for these conditions the flow stream may either be laminar or in transition. To account for these possibilities two equations were added to cover the range of Reynolds numbers found with low flow rates. First, for flow in the laminar region, the following equation is used for the Nusselt number:

$$Nu = 3.66 \tag{2.3.7}$$

This equation is valid for fully developed laminar flow inside a circular tube with constant wall temperature. Equation 2.3.7 is from Ozisik [11]. The use of this equation assumes a

constant wall temperature over the short section of tube for which the calculation is made.

For flow in the transition region a linear interpolation of the Nusselt number is taken between the value of Nu in the laminar region (Re=2300) and the value of Nu at the onset of complete turbulence (Re=10,000).

2.4 Exterior Heat Transfer Coefficient

Subroutine OUTSIDE calculates the exterior heat transfer coefficient given the diameter of the tube, the wall and storage temperatures. The exterior heat transfer coefficient for natural convection from a horizontal tube is the parameter which is most difficult to calculate, and is the most unique parameter for each heat exchanger. Natural convection from the exterior of the heat exchanger was found to contribute between 30% and 40% of the resistance to overall heat exchange. This fact makes it important from a modeling standpoint to accurately characterize this portion of the heat transfer.

The construction of the heat exchangers, various shapes and orientations of coiled tubing, provide the starting point for a heat transfer correlation. The heat transfer coefficient is obtained from the Morgan [7] correlation for the average Nusselt number as a function of the Rayleigh number for an infinitely long tube in an infinite medium, which takes the

following form:

$$\overline{Nu_D} = C\ Ra_D^m \qquad (2.4.1)$$

where

$$Ra_D = \frac{g\ \beta\ (T_w - T_s)\ (OD)^3}{\nu\ \alpha} \qquad (2.4.2)$$

and the ranges for the constants C and m are as follows:

Ra_D range	C	m
10^{-10} - 10^{-2}	0.675	0.058
10^{-2} - 10^{2}	1.020	0.148
10^{2} - 10^{4}	0.850	0.188
10^{4} - 10^{7}	0.480	0.250
10^{7} - 10^{12}	0.125	0.333

Both Feiereisen and Farrington use the form of the Morgan correlation with m = 0.25 and C a variable constant to express their experimental results. Also, Sparrow and others [14,15] have experimentally verified the correlation for heat transfer from an infinitely long tube in an infinite medium. The properties of the heat transfer fluid are evaluated at the film temperature, an average of the wall and tank temperatures. The heat transfer coefficient is then found from:

$$h_o = k\ \frac{\overline{Nu}}{OD} \qquad (2.4.3)$$

The Morgan correlation is used as a starting point

for describing natural convective heat transfer from an immersed heat exchanger. The correlation does not, however, completely encompass the situation for heat exchangers, as a coiled tube placed inside an enclosure deviates significantly from the assumptions of the Morgan correlation. First of all, the tank enclosure violates the infinite medium assumption as natural convection currents are set up inside the tank when heating takes place. The wrapped nature of the tubing violates the infinitely long tube assumption, and the natural convection currents from the lower sections of the coil has an effect on the heat transfer from the upper part of the coil. Adding to the complexity of the geometry is the fact that most of the heat exchangers are constructed by hand without close dimensional tolerances, so small deviations in exterior geometry due to construction which have a significant effect on natural convection cannot be accounted for in a calculation of heat transfer. An example is the construction of the finned bayonet heat exchangers used by Farrington, which are wrapped as tightly as possible to maximize the heat transfer area per unit volume. All of these reasons contribute to an inability to calculate an exterior heat transfer coefficient.

The fact that the natural convection currents from the bottom of the coil affect the heat transfer from the upper part of the coil means that another phenomenon, that of enhancement of the natural convection heat transfer, is occurring. A number of studies [13-16] show that enhancement and/or

degradation occurs when heat is transfered from a bank of tubes by natural convection. The underlying theory is that when natural convection occurs from a tube a thermal and hydrodynamic wake is set up as bouyant forces move fluid upward past the tube. The temperature of the water in the wake is higher than the rest of the medium and it also has an upward velocity. Any tubes which are placed in this wake will be affected by the increased temperature and velocity of the surrounding fluid. Enhancement refers either to the enhancement or degradation of heat transfer from the affected tubes due to the wake. Two competing effects are taking place. The increased velocity of the fluid adds a little forced convective heat transfer. The temperature difference, however, is not as great and this retards heat transfer.

These studies have demonstrated different regions of action in the wake. If a second tube is very close to the bottom tube in a bank the thermal effects of the wake dominate and the convective heat transfer is less than if the affected tube stood alone. If the tube in the wake is placed further above the bottom tube hydrodynamic effects take over and the heat transfer is enhanced to a point where it is greater than a tube standing alone. As the affected tube is moved farther away from the bottom tube, eventually to infinity, the influence of the wake is gradually reduced to the point where it has no effect.

The characteristics of the wake depend on a number of factors, including tube spacing, end effects, the dimensions of the enclosure and any hydrodynamic effects due to the fins. Transient plumes have also been observed by Farrington [5] with one of the configurations. The experimental work on enhancement effects up to the present time have considered only idealized conditions, as most of the experiments were carried out using electrically heated tubes with air as the heat transfer medium. The cylinders also were made to approximate the infinite length assumption. The work, therefore, does not lend itself to application for complex exchanger geometries.

It follows that a direct calculation of the enhancement effects, at this time, is not possible. First, there is not enough experimental data for complex heat exchanger geometries upon which to base analytical calculations of enhancement. Second, the problems associated with the irregular geometry and the manufacture of the heat exchangers reduce the possible accuracy of any analytical calculation of the exterior heat transfer coefficient. The enhancement of natural convection heat transfer, then, can only be found experimentally for each exchanger-tank configuration.

A single multiplicative constant M, included in the Morgan correlation, has been found to adequately compensate for any enhancement and/or degredation of the natural convection. Mathematically this was the easiest way to include physical conditions about which little is known. A single value of M

for each heat exchanger geometry proved to be an adequate adjustment to the Morgan correlation to take into account all the deviations from the original assumption of an infinitely long tube in an infinite medium. One value of M for each heat exchanger was sufficient to predict heat flow very close to the heat flow measured in the experiment. The value of M was determined by fitting the simulated heat exchanger exit temperature to that of the experimental data in each case. The adjustment to the Morgan correlation takes the following form:

$$\overline{Nu_D} = M\ C\ Ra_D^{\ m} \qquad (2.4.4)$$

It must be noted here that M is an average enhancement factor over the entire length of the heat exchanger, though the Rayleigh number and the thermal conditions change along the length of the heat exchanger.

2.5 Heat Exchangers with Fins and/or Double Wall Construction

Fins and double walls present two problems not covered in the general Nusselt correlations. The mathematical treatment of each of the cases is described in this section.

Fins on a heat exchanger serve to increase the heat transfer area without increasing the length of the exchanger. Two parameters describe the significance of the fins, the total exterior heat transfer area A_o and the fin efficiency η. The

fin efficiency is found as a function of the fin geometry and the exterior heat transfer coefficient. As the exterior heat transfer coefficient decreases the fin efficiency increases. The method of calculating a fin efficiency can be found in Incropera and DeWitt [10a]. Farrington found that fin efficiencies varied between 0.66 and 0.93 for the three finned heat exchangers he tested. The fin efficiency range was found as a function of the exterior heat transfer coefficient, which was varied from 200 W/m^2 K to 1200 W/m^2 K. This range of h_o was found to be typical for the simulations of each of the finned heat exchangers. An average value of 0.8 is used in formula 2.5.1. A_o includes the portion of the smooth tube exposed and the total area of the fins. The fraction of the heat transfer area due to the fins is also usually specified as A_f. An adjusted or effective total exterior heat transfer area A_ε can then be calculated using the formula:

$$A_\varepsilon = A_o \left((1.0 - A_f) + A_f \eta\right) \qquad (2.5.1)$$

It is assumed that the Morgan correlation for the Nusselt number for the exterior of the heat exchanger applies to the fin surfaces as well, and that the constant M accounts for any variability in the average Nusselt number due to hydrodynamic effects caused by the fins.

Double wall construction in heat exchangers is a common method of protecting potable water supplies from any contaminants in the collector fluid loop. Double wall

construction also adds resistance to heat transfer through the exchanger wall, and must be accounted for in the model. Two parameters which describe the contact are the contact diameter CD and the contact coefficient h_c, which is specified as an exchanger parameter. Feiereisen measured the contact coefficient for double wall heat exchanger types 1, 2 and 4 and found values of h_o between 1300 W/m^2 C and 4000 W/m^2 C. A value of 2200 W/m^2 K was used for the double wall bayonet heat exchanger tested by Farrington. Assuming the contact coefficient is known a contact resistance R can be calculated and included in the calculation of the UA for the tube:

$$R = \frac{1}{h_c A_c} \qquad (2.5.3)$$

where A_c is the contact area:

$$A_c = \pi \, CD \, L \qquad (2.5.4)$$

The UA for any length of tube is then calculated as:

$$UA = \frac{1}{\frac{1}{h_o A_e} + \frac{1}{h_i A_i} + R} \qquad (2.5.5)$$

This method may also be used to include any resistance due to the wall construction that may occur.

2.6 Steady State Heat Transfer Calculation

For each discrete time step the program calculates a steady state heat transfer from the entire heat exchanger. In order to take into account any significant drop of collector fluid temperature inside the exchanger the length of the exchanger in the BENCHMARK program is divided into 30 sections (this is an arbitrary number: later investigation showed that simulations based on as few as 5 sections performed adequately.) Each section has a separate calculation of heat flow. A diagram of a typical tube section is shown in figure 2 in section 2.7, along with all the mathematical parameters in the energy balance equations. Subroutine SIMULATE governs the steady state calculation. Each section of tubing, starting with the tube section at the heat exchanger inlet, has its thermal parameter unknowns, wall temperature and exit temperature, solved by the equation solving subroutine TWALL, which is detailed in section 2.7. Once the thermal conditions are known, the heat transfer parameters such as heat transfer coefficients, heat flow and a section UA can be calculated for the particular section. The exit temperature of the section in question then becomes the inlet temperature for the following section. When the end of the tube is reached the heat flow is summed for the whole heat exchanger, and this value, along with the effectiveness, is returned to the main program for that time step.

2.7 Equation Solver

Subroutine TWALL solves a system of four equations which represent the heat flow from the section in question. The four equations are solved for the unknown exit temperature T_o and wall temperature T_w. A typical section looks like the following:

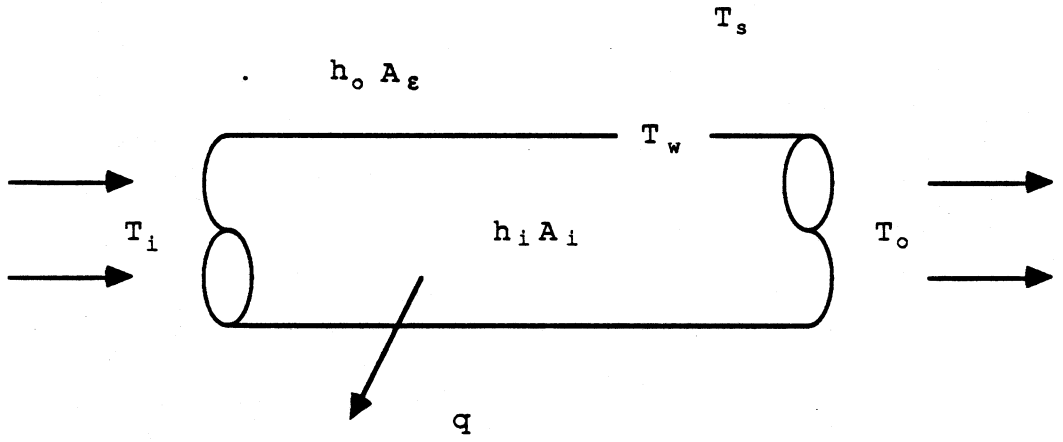

Figure 2. Schematic for tube section showing thermal parameters.

For purposes of heat flow calculation it will be assumed that the interior temperture, T_{ref}, is constant along the length of the section and equal to the average of the inlet and exit temperatures:

$$T_{ref} = \frac{T_i + T_o}{2.0} \qquad (2.7.1)$$

Four equations each represent the heat flow for each section:

$$q = h_o A_\ell (T_w - T_s) = UAI(T_{ref} - T_w) \qquad (2.7.2)$$

and

$$q = \dot{m} C_p (T_i - T_o) = UA\,(T_{ref} - T_s) \qquad (2.7.3)$$

where

$$UAI = \frac{1.0}{\frac{1.0}{h_i A_i} + R} \qquad (2.7.4)$$

and UA is defined in equation (2.5.5). The four equations shown above can be reduced to two equations representing the two unknown temperatures:

$$T_{wnew} = \frac{h_o A_\ell\, T_s + UAI\, \frac{T_i + T_o}{2.0}}{h_o A_\ell + UAI} \qquad (2.7.5)$$

and

$$T_{onew} = \frac{\dot{m} C_p\, T_i + UA\, T_s - \frac{UA\, T_i}{2.0}}{\frac{UA}{2.0} + \dot{m} C_p} \qquad (2.7.6)$$

The subroutine uses a successive substitution method to solve for the unknown temperatures for each section using initial guesses for both T_w and T_o. Successive substitution is successful because the property values are relatively unresponsive to small changes in temperature. Also, the Rayleigh number is dependent on the wall temperature to the 0.25 power. These equations are used to calculate new values for T_w and T_o, which

in turn become initial guesses until they change less than 0.0001 K. These values are then returned to subroutine SIMULATE, which is then able to calculate the heat transfer given the known thermal conditions for the tube section.

2.8 Main Program

The main program has been structured in such a way as to simulate an experimental run for a heat exchanger as was done by Farrington [5]. The main program solves an energy balance on the storage tank for each time step given the steady state heat transfer caluculated in subroutine SIMULATE. The main program also calculates such heat exchanger variables such as the overall UA and the log mean temperature difference.

2.9 Simplified Programs

A simplified program is required to satisfy computing restraints in large simulation packages [2]. The reduction in computing requirements results from the elimination of one or more of the iterative loops used in the program. Two simplified versions were developed. The program SIMPLE utilizes an average UA and therefore does not require the calculation of UA for each section. This simplification

eliminates the position dependence of the calculations, and therefore SIMPLE does not require the successive substitution solution to equations 2.7.2 and 2.7.3. A constant effectiveness program called CONSTE calculates an effectiveness for the heat exchanger given the initial thermal conditions. The effectiveness is then used to calculate all the steady state heat flows, eliminating the time dependence in the solution and the second major iterative loop in the model.

The constant UA program uses an average UA for the entire tube to calculate the steady state heat transfer. An early perusal of results from the benchmark model showed that the value of UA changed between 8% and 40% along the length of the tube in the four heat exchangers modeled. In the constant UA program an average UA for the entire tube is calculated from the arithmetic average of UA at the beginning and end of the tube. This assumes that the value of UA varies linearly along the length of the tube. Sections at the beginning and end of the tubes, each one hundredth the length of the entire tube, are used to calculate two values for UA from which the average is taken. The short sections allow the elimination of the exit temperature in the energy balance equations solved by subroutine TWALL, as it is assumed that the temperature drop is negligible over such a short distance. The shortened sections are pictured in figure 3.

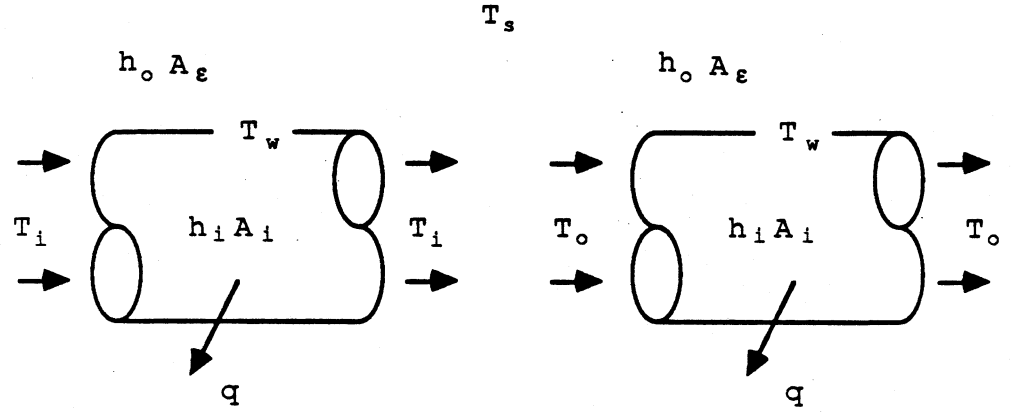

Figure 3. Shortened sections for average UA calculation thermal parameters.

The set of energy balance equations to be solved by subroutine TWALL for the single unknown temperature T_i or T_o reduces to two:

$$q = h_o A_\varepsilon (T_w - T_s) \qquad (2.9.1)$$

and

$$q = UAI(T_i - T_w) \qquad (2.9.2)$$

A successive substitution algorithm in subroutine TWALL is used to solve the following equation for T_w:

$$T_{wnew} = \frac{UAI\ T_i + h_o A_\varepsilon\ T_s}{UAI + h_o A_\varepsilon} \qquad (2.9.3)$$

Subroutine SIMULATE uses a successive substitution loop to converge on the average UA value. This loop is necessary because the exit temperature for the heat exchanger is not

known at the beginning of the calculation for UA. This exit temperature is estimated to start with, from which an initial average UA is calculated. The UA value is used to find the actual exit temperature using the NTU relation for heat exchanger effectiveness, shown in the following equations:

$$NTU = \frac{UA}{\dot{m}\, C_p} \qquad (2.9.4)$$

and

$$\varepsilon = 1.0 - e^{-NTU} \qquad (2.9.5)$$

the exit temperature is then found from:

$$T_{onew} = T_i - \varepsilon\,(T_i - T_s) \qquad (2.9.6)$$

The successive substitution loop in subroutine SIMULATE cycles until the exit temperature changes less than the value of $0.001(T_i - T_o)$. The effectiveness can then be used directly to calculate the steady state heat flow.

The constant effectiveness program utilizes the same subroutines SIMULATE and TWALL for calculating UA as the simplified program, but simulates the heat exchanger for only the initial time step, using that calculated effectiveness to calculate heat transfer at all future time steps. The only difference between this model and the constant UA model is that the subroutine SIMULATE is called only once, as it is removed from the iterative loop over time. The initial call to subroutine SIMULATE is just a way of estimating the effectiveness given the temperature conditions, flowrate and physical dimensions of the heat exchanger. If an effectiveness could be

guessed without the use of subroutine SIMULATE the program would be reduced to a trivial algorithm.

3.0 Results

The performance of the model can be demonstrated by comparing the system variable values during a simulation with those actually measured in the companion experiment. The calculation of heat flow and other heat exchanger parameters by each of the programs has been compared with the experimental data generated by Farrington. Experimental data of this kind is difficult to obtain, and this validation, though limited, is the best that could be done.

This section contains plots of experimental versus simulated data, covering such parameters as system temperatures, heat flows and effectivenesses. There are also more direct comparison data, some error estimations for each model and information concerning the factor M for heat exchangers examined by Feiereisen [4] and Farrington [5].

3.1 Experimental Data

The experimental work by Farrington [5] resulted in data for four heat exchangers, each of which were tested at three flow rates. The heat exchanger types were (5) a smooth tube coil in the shape of a cylinder, (6) a finned coil which spiraled up at a decreasing diameter, and two finned bayonet

style heat exchangers, one with single wall construction (7) and the other double wall construction (8). The same cylindrical, 409 liter storage tank was used for each of the experimental runs. The original experimental data consisted of heat exchanger inlet and exit temperatures, four thermocouple measurements of tank temperature, and a mass flow rate for the hot side water. A diagram of the experimental apparatus can be seen in figure 4; it shows the hardware setup and thermocouple positions. Figures 4a through 4d are schematic drawings of each of the heat exchangers tested by Farrington. Additional experimental data were calculated, including heat flow, effectiveness and heat exchanger UA. The heat flow was calculated from an energy balance on the hot side fluid:

$$Q = \dot{m}\, C_p\, (\, T_i - T_o\,) \qquad (3.1.1)$$

The LMTD was found from:

$$LMTD = \frac{T_i - T_o}{\ln \dfrac{T_i - T_s}{T_o - T_s}} \qquad (3.1.2)$$

The heat exchanger UA is then calculated:

$$UA = \frac{Q}{LMTD} \qquad (3.1.3)$$

Finally, the effectiveness is calculated from:

$$\varepsilon = \frac{T_i - T_o}{T_i - T_s} \qquad (3.1.4)$$

All the experimental data were tabulated versus time.

The heat exchanger inlet and exit temperatures formed the basis for the comparison with the programs. The heat flow for the experimental data was calculated using the inlet and exit temperature difference and the measured mass flow rate. This was done in order to minimize the effects of experimental error, as only two thermocouples and one flow rate were involved in measuring the necessary data. The heat flow calculated in this manner did not agree with the heat flow calculated from an energy balance on the storage tank. The tank temperature predicted by the programs usually does not agree with that from the experimental data, and this should not be seen as a weakness in the model. The error in the storage temperature shows this energy imbalance, and this can be seen in the plots of temperature data in this Chapter.

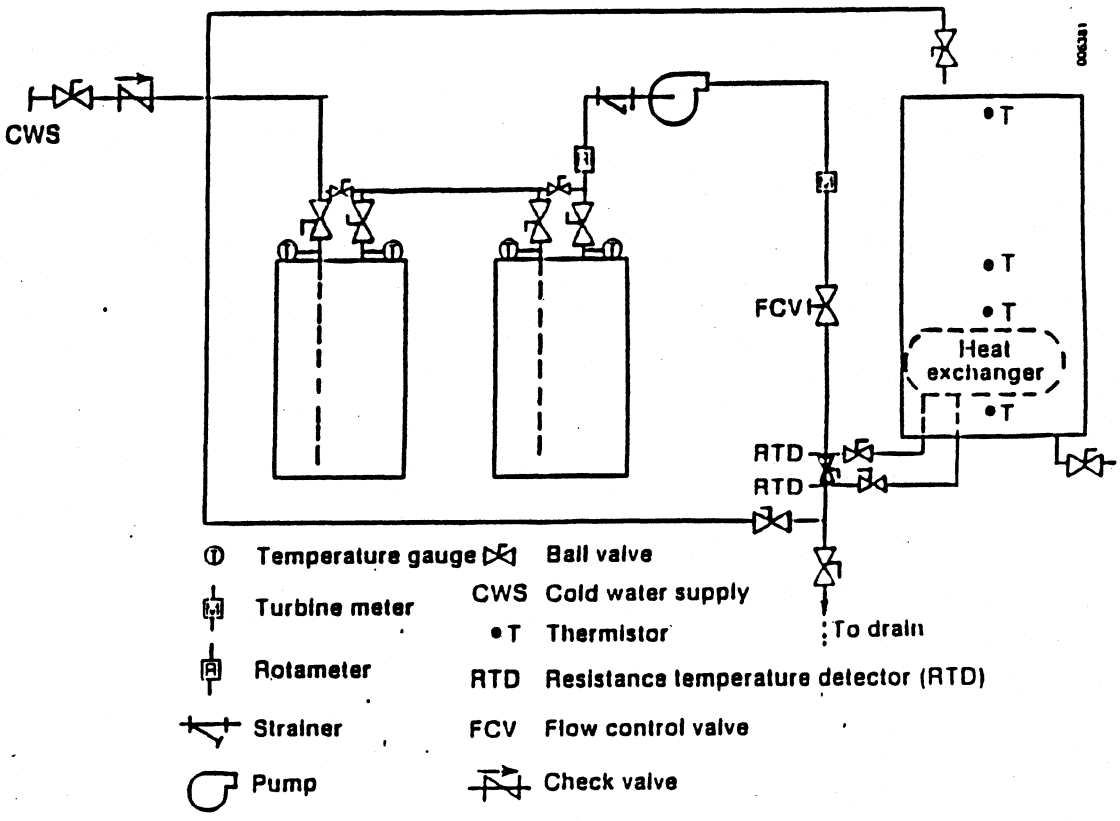

Figure 4. Experimental Equipment Schematic (Farrington [5])

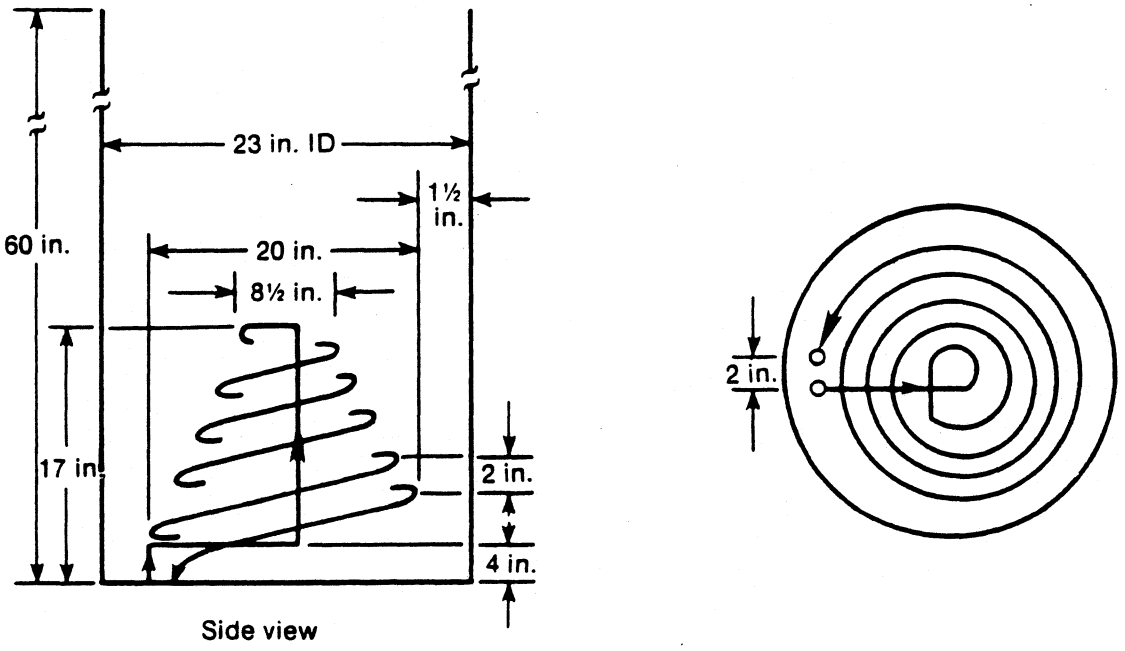

Figure 4a. Finned Spiral Heat Exchanger Schematic (Farrington [5])

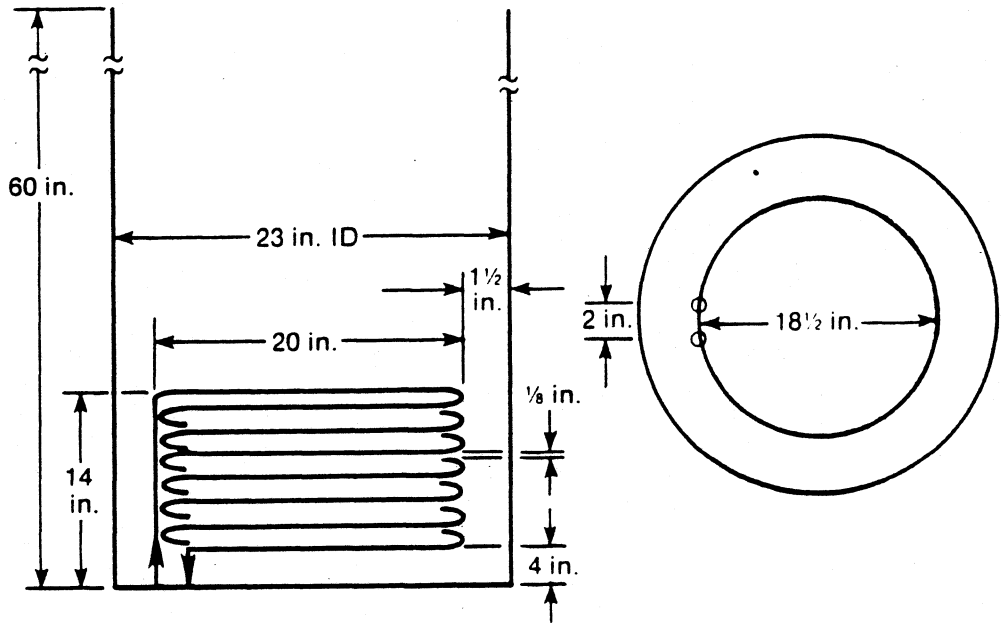

Figure 4b. Smooth Coil Heat Exchanger Schematic (Farrington [5])

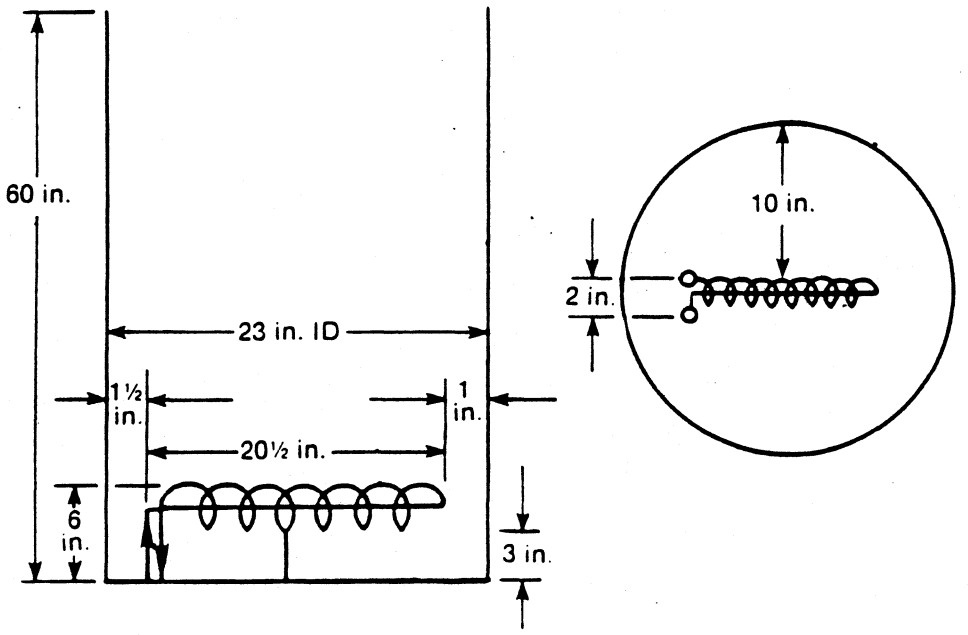

Figure 4c. Single Wall Bayonet Heat Exchanger Schematic (Farrington [5])

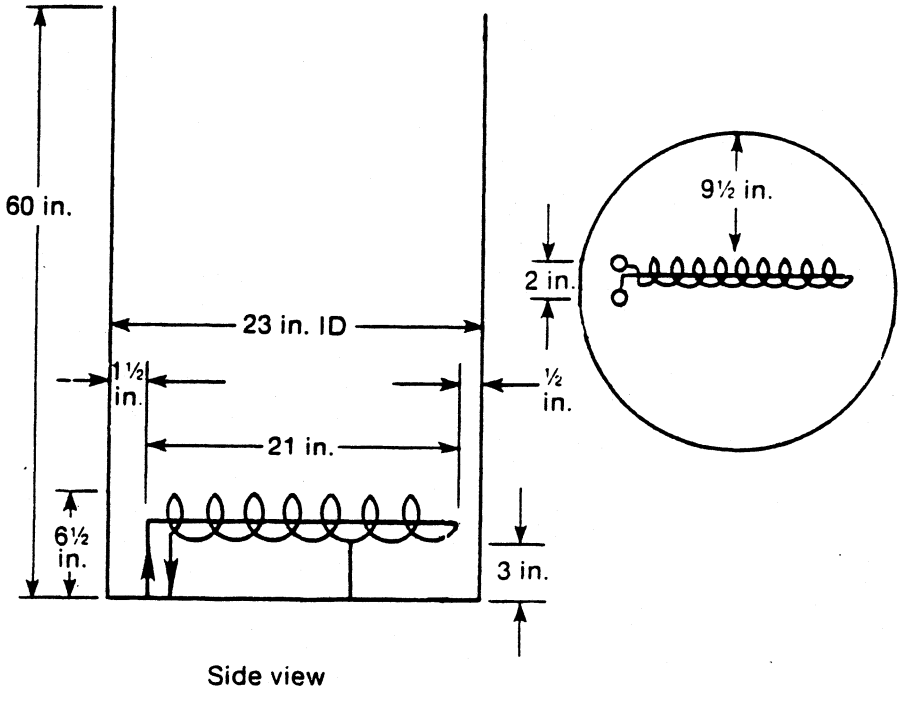

Figure 4d. Double Wall Bayonet Heat Exchanger Schematic (Farrington [5])

3.2 M Values

Table 1 shows the value of M for the four heat exchangers investigated by Farrington (heat exchangers 5-8). These values were found by trial and error, adjusting the value of M used in the Morgan correlation until the heat exchanger exit temperature calculated by the simulation was as near as possible to the exit temperature measured by Farrington. This was done for each heat exchanger test reported by Farrington. A single value of M was then found for each heat exchanger, and this value of M resulted in accurate heat flow predictions at all three flow rates used by Farrington. The procedure used to find M is shown in figure 8 in section 3.3, which shows the simulated exit temperature for the finned spiral heat exchanger test at a 15 l/min flow rate. The value of M is 1.0 in this simulation and the simulated exit temperature is much higher than the measured exit temperature. Figure 6 shows the same test where M is 1.8 and the simulated exit temperature is close to the measured exit temperature. Also shown in Table 1 are values of M for the four heat exchager configurations examined by Feiereisen (heat exchangers 1-4). The values for M here were found from the Nusselt-Rayliegh correlations presented by Feiereisen, and the range of the value M in the observed correlation demonstrates the difficulty in determining exact, consistent measurements of natural convection heat transfer.

Heat Exchanger	M	Range of Measurement (Variation of Observation)
One Horizontal Multi Pass Smooth Tube Coil(1)	0.77	0.50 < M < 1.125
Horizontal Spiraling Finned Tube Coil(2)	0.71	0.46 < M < 0.92
Horizontal Single Pass Smooth Tube Coil(3)	1.54	1.02 < M < 2.215
Two Horizontal Multi Pass Smooth Tube Coils(4)	1.15	0.88 < M < 1.56
Smooth Tube(5)	1.30	
Finned Spiral(6)	1.80	
Single Wall Bayonet(7)	1.35	
Double Wall Bayonet(8)	1.70	

Table 1. M Values for Each Heat Exchanger

3.3 Model vs. Experiment

Simulations of the tests done by Farrington were carried out using the heat exchanger inlet temperatures and mass flows measured by Farrington. The programs predicted heat exchanger exit temperatures, tank temperatures and values for the heat flow Q, the effectiveness and overall exchanger UA. Farrington generated data for 12 experimental runs altogether, testing each of the four heat exchangers at mass flow rates of 5, 10 and 15 liters per minute. Performance data for simulations of all the experiments using each of the three programs will be examined in the next section.

Figures 5, 6 and 7 show the performance of the BENCHMARK program against the experiment in simulating the test of the finned spiral (6) heat exchanger with a mass flow rate of 15 liters per minute. This experimental run was chosen as representative of the test each heat exchanger was put through, and it will be used as a basis for an explanation of a more complete statistical analysis of the three programs. The simulated data in figures 5-7 is plotted along with the experimental data. The experimental data curves are generally irregular, reflecting the experimental noise, while the curves of simulated results are smooth.

Figure 5 is a plot of experimental and simulated heat flows versus time for the test of the finned spiral heat

exchanger (6) using a 15 liter per minute flow rate. The experimental heat flows were calculated from an energy balance on the hot side fluid flow. The change in experimental tank temperature did not equal the heat flow calculated from the heat exchanger, however, and the reasons for this energy imbalance are unknown. Possible sources of error may have been inaccurate thermistor measurements of tank temperature or inaccurate RTD measurements of the hot side fluid temperature. The error may also have resulted from a wrong assumption in the simulation of the storage tank loss coefficient. No energy balance was done on the data at the time of the experiment. The final experimental energy flow data was taken from an energy balance on the hot side of the heat exchanger. This was done in order to minimize the possible sources of error in the heat transfer calculation. Two RTD devices were used to measure the inlet and outlet temperature on the heat exchanger. The tank temperature measurement was taken as an average of the temperatures found from four thermistors located vertically down the center of the tank. The tank itself was also subject to movement when heat exchangers were changed, thus adding possible sources of error to the tank temperature measurement. The heat flow curves provide an idea of the accuracy of the model in predicting heat flows, and the overall accuracy of each of the programs in simulating each test is judged by these plots, as will be shown in the next section.

Figure 6 is a plot of system temperatures versus time. The temperatures are denoted by TI, TO and TS, which represent the heat exchanger inlet temperature, exit temperature and storage temperature, respectively. The inlet temperature for both the simulation and the experiment are identical, and this is shown by a single inlet temperature curve. The dropoff in the inlet temperature curve is due to a loss of thermal energy in the two hot water source tanks shown in figure 4 as the test tank is heated up. The simulated heat exchanger exit temperature curve follows the experimental data curve closely, as this is the curve which was fit by finding an appropriate value for M, the natural convection enhancement factor. The simulated tank temperature is shown along with the experimental tank temperature. The simulated tank temperature rises faster than the experimental tank temperature and the final simulated tank temperature is higher that the experimental tank temperature at the end of the test run. This difference between the simulated and experimental tank temperature occurs in each of the test runs, and it is a result of the energy imbalance discussed in the previous paragraph. The actual experimental heat flow is assumed to be found from an energy balance on the hot side fluid which means that the measurement of tank temperature is in error. The error may be occurring in the measurement of the hot side fluid temperatures or the mass flow, and the experimental tank temperature may be

accurate, but there is no indication which energy flow calculation is the correct one. The high simulated tank temperature results in a crossover of the inlet and tank temperatures, which is due to the fact that the inlet temperature in the simulation is taken from the experimental data while the simulated tank temperature is independent. The inlet temperature is influenced by the experimental tank temperature and not by the higher simulated tank temperature.

Figure 7 is a plot of simulated and measured effectiveness versus time. Again the effects of the assumed error in tank temperature can be seen in two characteristics of the plot. First of all the simulated effectiveness remains relatively constant while the measured effectiveness drops off, and this can be explained by a low measured tank temperature. Secondly, the abrupt change in the simulated effectiveness marks the point where the simulated tank temperature goes above the inlet temperature and the heat flow is reversed.

Figure 8 is a plot of system temperatures similar to figure 6 except that the natural convection enhancement factor M equals 1.0. This plot demonstrates the effect M has on each of the simulations and its importance in predicting heat flow. M values greater than 1.0 have an effect on calculated heat transfer in the range of high temperature differences and therefore high heat flows. Figure 8 shows a significant underprediction of heat flow without the use of the factor M. The value of M for each heat exchanger was found by fitting the

simulated exit temperature to the measured exit temperature in plots such as figure 8. The correct estimation of the value of M for the heat exchangers tested by Farrington depends on which calculation of the experimental heat flow is chosen as the correct one. Figure 8 shows that for M = 1.0 the simulated tank temperature is very close to the experimental tank temperature though the simulated exit temperature is much higher than experimental exit temperature. Again there is no indication which calculation of heat flow from the experimental data is the correct one.

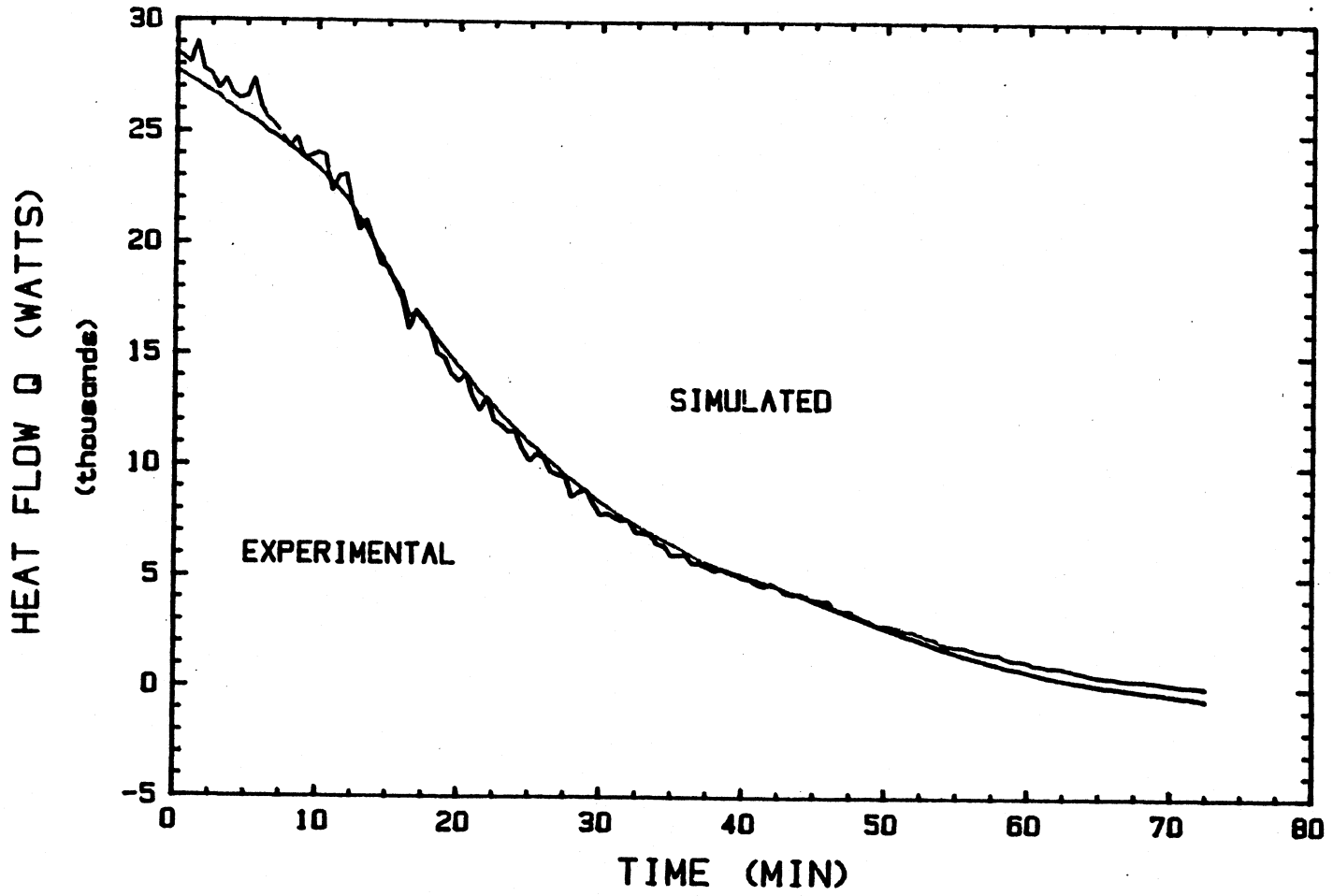

Figure 5. Finned Spiral heat exchanger test at 15 liters per minute; heat flow. Experimental data from Farrington [5].

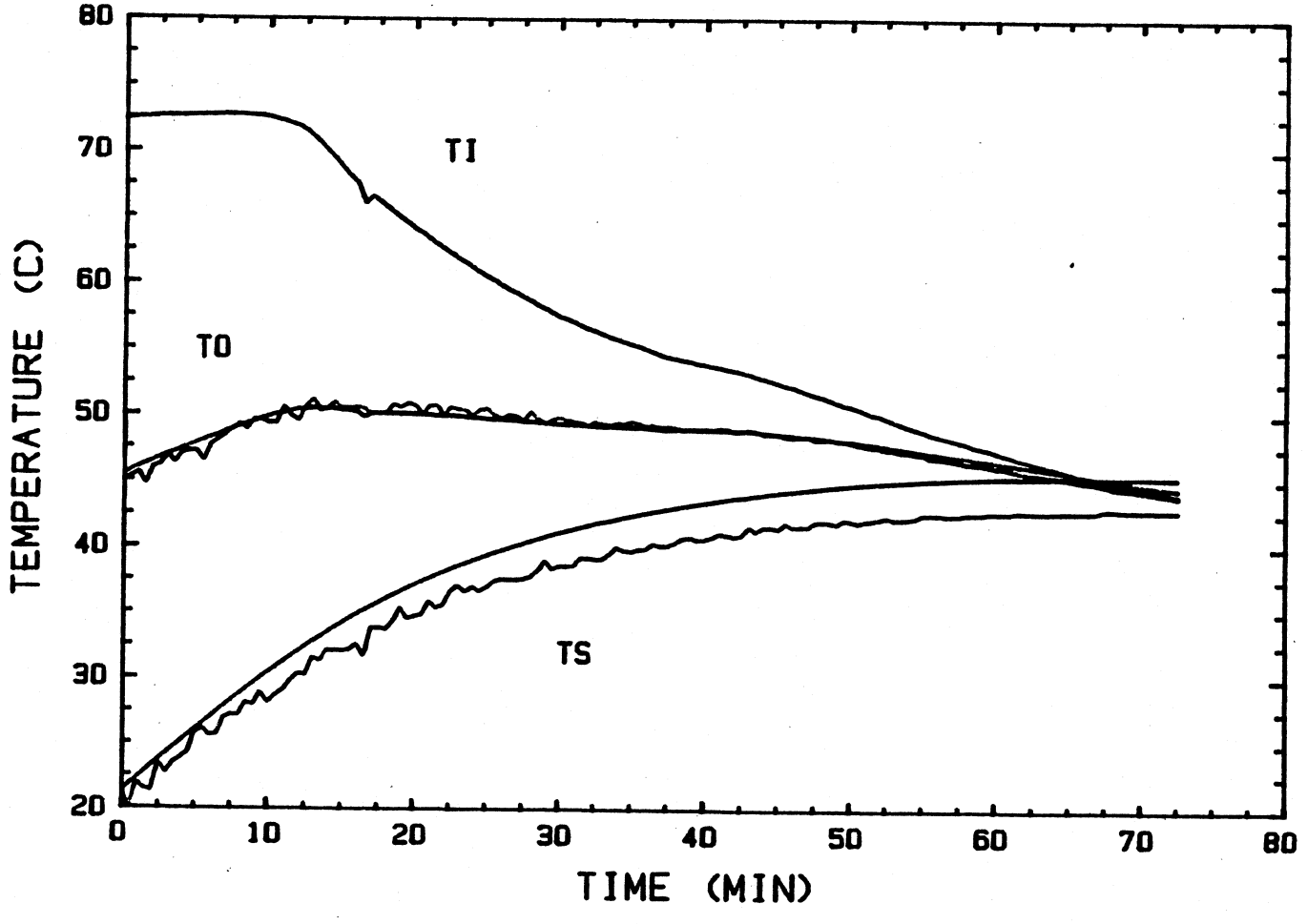

Figure 6. Finned Spiral heat exchanger test at 15 liters per minute; temperatures. Experimental data from Farrington [5].

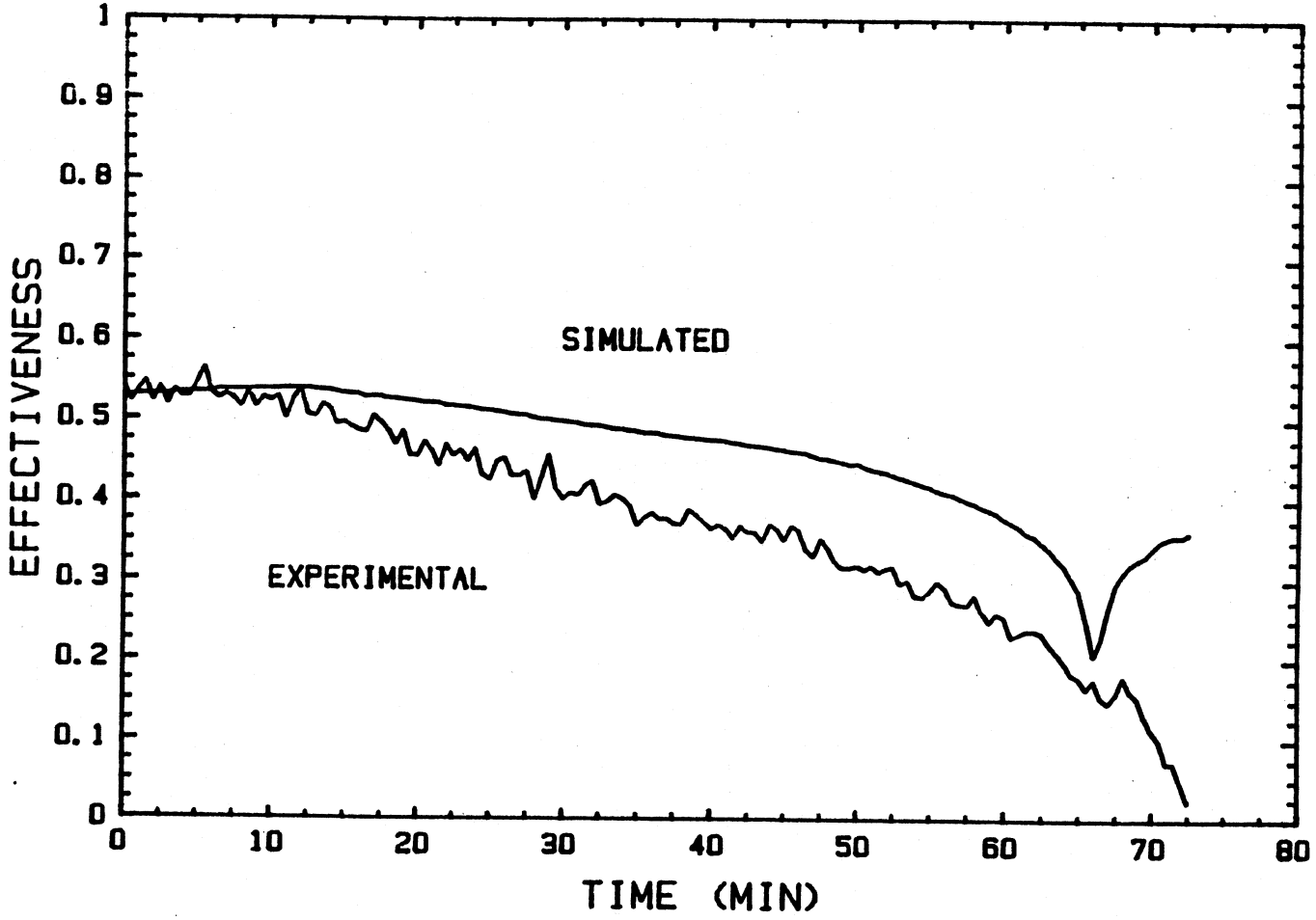

Figure 7. Finned Spiral heat exchanger test at 15 liters per minute; effectiveness. Experimental data from Farrington [5].

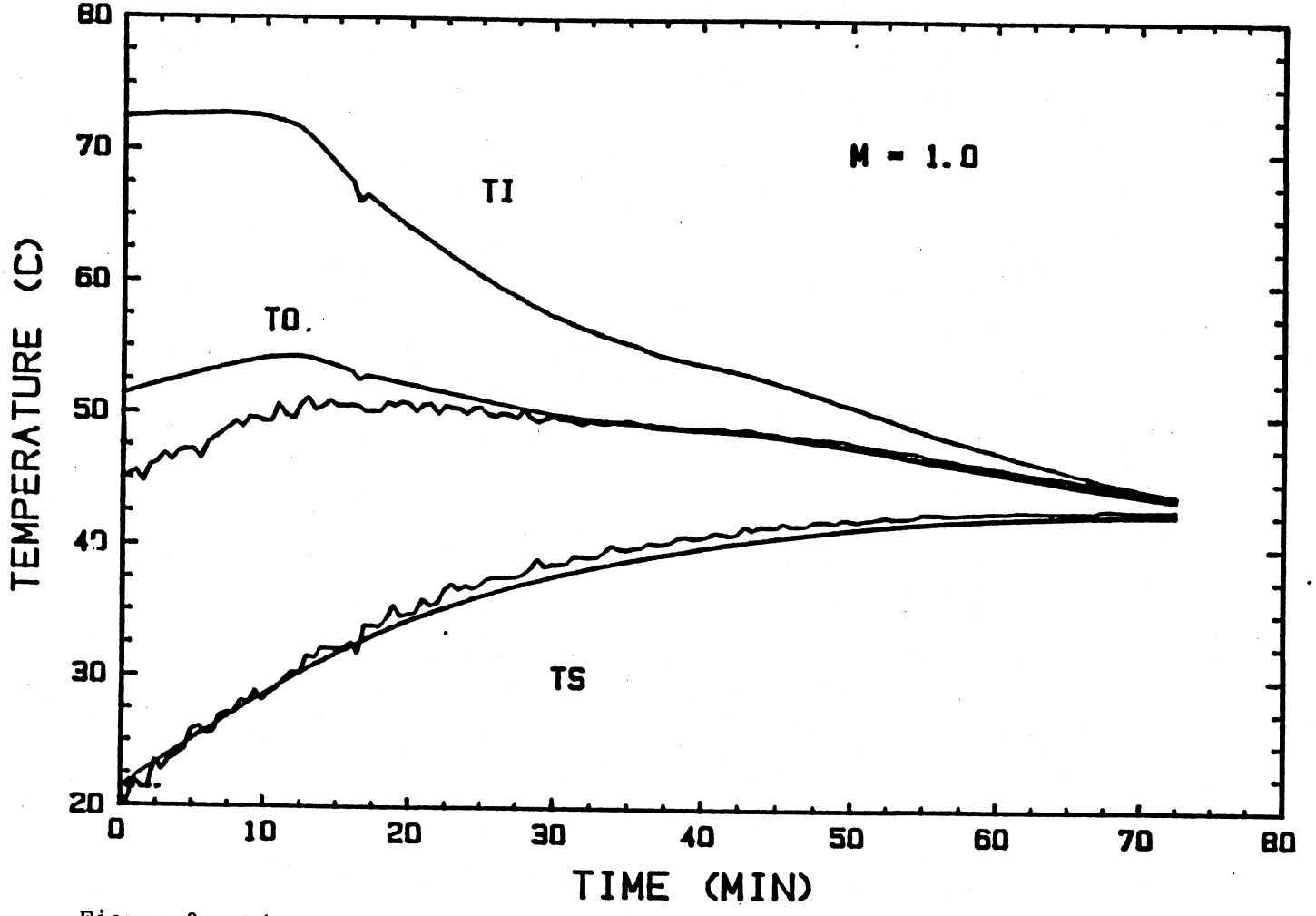

Figure 8. Finned Spiral heat exchanger test at 15 liters per minute; temperatures. Experimental data from Farrington [5], enhancement factor M = 1.0.

3.4 Analysis of Model Performance

This section presents a more complete analysis of the results of the performance of the three simulation programs. A statistical analysis will be presented in the next paragraph. First, however, figure 9 represents a survey of simulated versus experimental heat flows from each of the 12 tests conducted by Farrington. Three data points were selected from each test representing low, medium and high heat flows. There are 9 data points from the simulation of each heat exchanger, 36 points in all. This plot provides an idea of the accuracy of the model in predicting a wide range of heat flows from a variety of immersed heat exchangers.

Tables 2 and 3 present a statistical analysis of the performance of each of the programs in predicting the experimental heat flow. The experimental data points were taken at 0.5 minute intervals and resulted in erratic curves for heat flow results. This erratic behavior of the heat flow results can be called the experimental noise. A fifth order curve fit was made for the heat flow curves in order to eliminate the erratic nature of the experimental data from the calculation of standard deviations. The curve fit of the data was then considered the experimental heat flow to which the simulated heat flows could be compared. The curve fits were done using the Minpack subroutine LMDIF1 [8] for the heat flow results from

each of the test runs. A standard deviation and a bias error were then calculated for the experimental data and all three program simulations of heat flow against the curve fit to the experimental data. The standard deviation of the simulated heat flow will then be compared with that of the experimental heat flow to determine the how accurate the simulation is in predicting experimental heat flow. The standard deviation is calculated in the following way:

$$\sigma^2 = \frac{\sum_{i=1}^{N} (Y_i - \bar{Y}_i)^2}{N - P} \qquad (3.4.1)$$

where $\bar{Y}_i$ is the heat flow from the fitted curve and Y_i is either the original data heat flow or the simulated heat flow. P in equation (3.4.1) is the number of data points and N is the number of parameters used for the fitted curve to the data. For the experimental standard deviation P=6 for the fifth order polynomial. The simulated heat flow standard deviation had P=0 since the fitted curve was not related to this data. The value of N was typically between 100 and 150, so the effect of a small P is diminished. The performance of the programs can be judged when the standard deviation of the simulation is compared with the standard deviation of the experimental data. If the two quantities are nearly equal then the errors in the simulated heat flow fall within the bounds of the experimental noise. This result would mean that the simulation is as good as the experiment in predicting heat flow. If the standard

deviation of simulated errors is greater than the experimental noise, then there is a significant error attributable to the model.

The bias error is a measure of whether the error is above or below the curve fit of experimental heat flow or centered on it. The bias error is usually very small for the data to which the curve is fit. The error is calculated in the following way:

$$\text{Bias} = \frac{\sum_{i=1}^{N} (Y_i - \bar{Y}_i)}{N - P} \qquad (3.4.2)$$

where the symbols correspond to those in equation (3.4.1). The statistical methods used can be referenced in Box, Hunter and Hunter [12]. The standard deviation of heat flow and bias error for each of the programs as well as the experimental data can be found in tables 2 and 3.

Tables 2 and 3 contain the standard deviation and bias error for the experimental data and all three simulation programs corresponding to each of the 12 experiments run by Farrington. The performance of each of the programs can be determined by comparing the standard deviation of the simulated heat flow with that of the experimental data for the same test. If the two standard deviations are nearly equal then the simulation error is within the experimental noise and the model results are an accurate prediction of the actual heat flow. The bias error column gives an idea of the positioning of the

errors. A negative bias means the simulation erred on the low side of the heat flow the majority of the time. A positive bias means the simulation simulation predicted too much heat flow a majority of the time. A bias of zero indicates the errors were centered about the fitted curve.

Tables 2 and 3 show that for most of the experimental runs the standard deviation of the simulated heat flow is greater than the standard deviation of the experimental heat flow. The magnitude of the errors in predicted heat flow for each test run can best be understood with an example. The finned spiral heat exchanger test results at 15 l/min flow rate are plotted in figures 5, 6 and 7. The simulated and experimental heat flows are plotted in figure 5. The simulation results in this plot were found using the BENCHMARK program. Figure 5 shows that the simulated heat transfer follows the experimental heat transfer closely. The standard deviation for the simulated heat flow in this experiment, found in table 2, is 482 Watts and the bias error is -135.7 Watts. The standard deviation for the experimental data about the fitted curve is 391.5 Watts. These data indicate that the simulated heat flow is in error greater than the experimental noise is from the fitted curve, and thus the error in simulated heat flow is significant. The negative bias error indicates that the majority of the simulated heat flows are lower than the experimental heat flows, and this can be verified with an examination of figure 5. The fitted heat flow curve is not shown in figure 5,

but the small bias error for the experimental data indicates the fifth order curve fit followed the experimental heat flow closely.

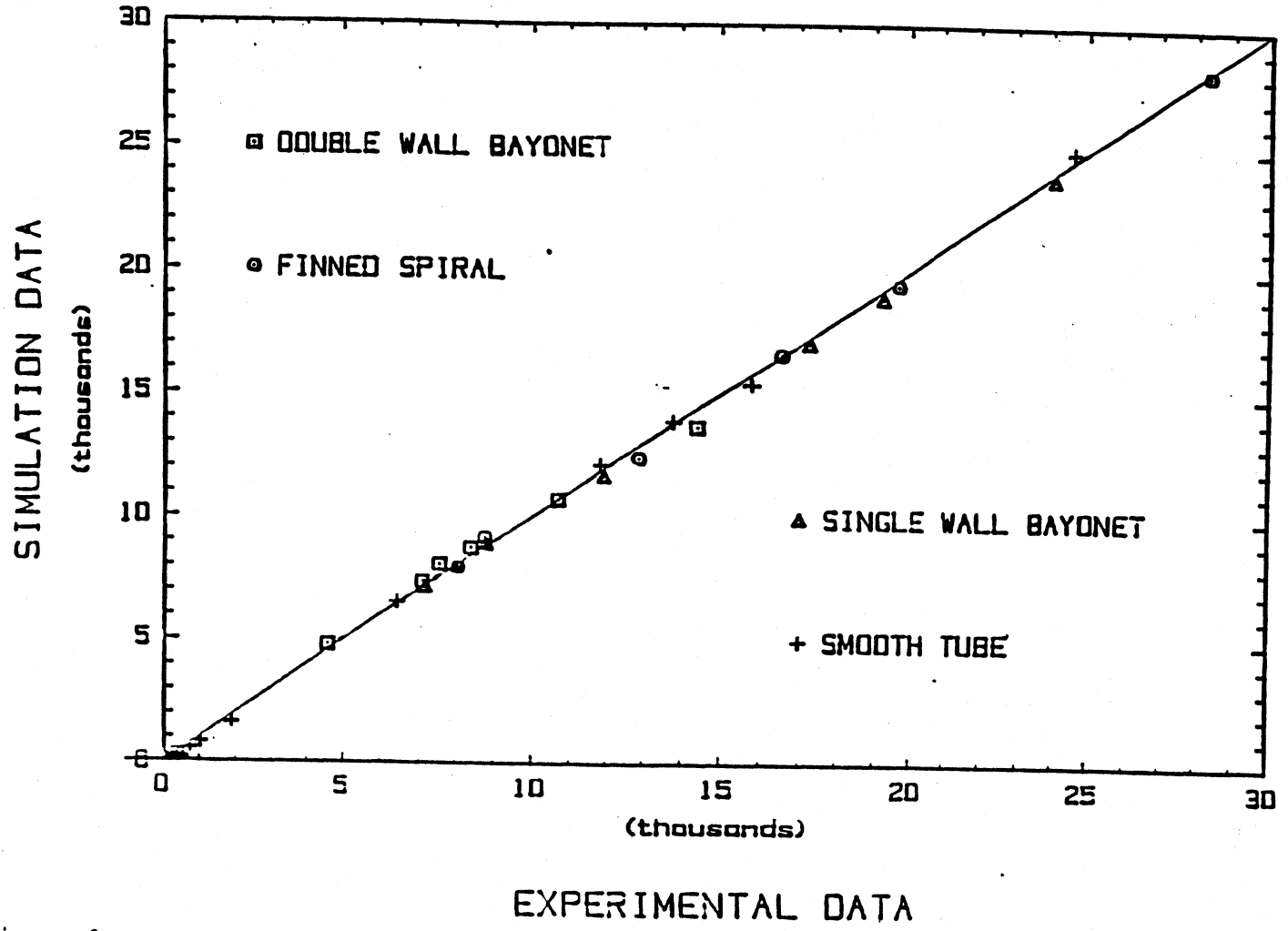

Figure 9. Survey of simulated vs. experimental heat flows; high, medium and low heat heat flows represented. Experimental data from Farrington [5].

Heat Exchanger	Flowrate L/Min	σ and Bias Error (Watts)			
		Experimental		BENCHMARK	
		σ	Bias	σ	Bias
Finned Spiral	15	391.50	4.09	482.00	-135.70
	10	126.50	-0.013	326.60	-218.50
	5	90.89	-1.30	233.19	-159.60
Smooth Tube	15	253.99	1.00	419.05	-394.3
	10	115.88	-0.051	135.06	-100.67
	5	77.63	-0.51	203.55	-164.37
Double Wall Bayonet	15	284.56	-4.46	501.00	150.60
	10	68.04	1.02	156.35	77.41
	5	55.95	-0.91	128.64	7.60
Single Wall Bayonet	15	547.86	3.98	649.87	214.70
	10	129.71	-1.50	200.04	-67.40
	5	95.43	-0.073	171.35	-53.71

Table 2. Statistical Comparison of Simulated and Experimental Data

Heat Exchanger	Flowrate L/Min	σ and Bias Error (Watts)			
		SIMPLE		CONSTE	
		σ	Bias	σ	Bias
Finned Spiral	15	454.50	-117.70	649.40	13.18
	10	313.60	-217.20	321.90	-211.40
	5	212.31	-156.00	239.92	161.00
Smooth Tube	15	426.79	-377.60	259.85	-200.47
	10	159.07	-91.85	153.50	25.86
	5	234.62	-154.90	201.19	-128.71
Double Wall Bayonet	15	501.20	150.4	548.90	163.30
	10	156.35	77.32	161.72	79.00
	5	128.55	7.52	95.84	6.46
Single Wall Bayonet	15	626.80	231.13	893.71	459.06
	10	182.09	-65.25	221.62	-34.85
	5	145.50	-50.65	210.76	-53.12

Table 3. Statistical Comparison of Simulated and Experimental Data

3.5 Yearly Simulations

A number of yearly simulations were performed to test the heat exchanger-tank model in a solar domestic hot water system. The yearly simulations were done for a solar system supplying domestic hot water to a family of four in Madison, Wisconsin. Each of the four heat exchangers tested by Farrington were used in the yearly simulations. The simulations were performed using both variable effectiveness models and constant effectiveness models, and the effect of M on the yearly performance of the system was investigated.

It was found that for the size heat exchangers tested by Farrington at standard flow rates (0.015 kg/m^2 s) the collector area penalty F_R'/F_R (defined by Duffie and Beckman [1]) is small enough such that an assumption of constant effectiveness leads to predicted system performance results which are nearly equal to those found from a variable effectiveness model. This can be seen in figures 10 and 11, where the yearly solar fraction found using a constant effectiveness model is compared to the yearly solar fraction found using a variable effectiveness model.

The fact that the immersed heat exchangers tested result in small collector area penalties means that the selection of a value of M, the natural convection enhancement factor, is not critical in the calculation of system per-

formance provided the value is within reasonable bounds. For instance, the value of M for the 8 heat exchangers examined in this thesis range from 0.71 to 1.8. Different values of M result in different effectivenesses calculated at set temperature conditions, which for this thesis means a 50 C difference between the inlet and tank temperatures. The magnitude of the difference in calculated effectiveness caused by a difference in the value of M can be seen in figure 12, which is a plot of constant effectiveness versus heat exchanger size for the single wall bayonet heat exchanger at a standard flow rate. The collector area penalty for the single wall bayonet heat exchanger tested, which was 4.9 m long, was found to be 3% for M=1.35 and 4% for M=1.0. A similar heat exchanger 2.5 m long would result in a 7% collector area penalty using m=1.35 and 9% penalty if M=1.0. These small collector area penalties do not affect yearly performance significantly, and this can be seen in tables 4 and 5, which contain solar fraction results for a sample of yearly simulations employing a number of collector flow rate combinations for the four heat exchangers tested by Farrington. Tables 4 and 5 show that for the four heat exchangers tested the solar fraction was not significantly affected by the value of M, and this is true for high, medium and low solar fractions.

Heat exchanger flow rate combinations whose collector area penalty is higher than 10% may lead to yearly performance estimates which are adversely affected by differences

in the value of M and those errors which are inherent in the selection of a constant effectiveness model. A high collector area penalty may be associated with a low flow rate or a small heat exchanger. The effect of small heat exchanger size on effectiveness is shown in figure 12 for the single wall bayonet heat exchanger. At standard flow rates the single wall bayonet heat exchanger has very low effectivenesses at lengths below 2 m, and this results in high collector area penalties. Systems with high collector area penalties require an accurate estimate of M and an appropriate selection of temperature conditions with which to calculate an effectiveness in order to obtain accurate yearly performance predictions.

Figures 10 and 11 present a comparison of the accuracy of using a constant effectiveness versus variable effectiveness model on the yearly simulated performance. Figure 10 is a plot of the solar fraction found using a constant effectiveness versus the solar fraction found using a variable effectiveness for the single wall bayonet heat exchanger. A range of flowrate-area combinations are shown here, and the value of M is 1.35, the experimentally determined natural convection enhancement factor. It is evident that the selection of a constant effectiveness for the heat exchangers tested provides solar fractions which are equivalent to those found using a variable effectiveness model in the simulation. Figure 11 demonstrates that the same conclusion is true for the results where M is removed from the calculation of the exterior

heat transfer coefficient. The single wall bayonet heat exchanger is representative of the four exchangers provided by Farrington. This result, coupled with the results found in tables 4 and 5 lead to the conclusion that an accurate estimate of the annual solar fraction using the heat exchangers tested by Farrington can be made by using a constant effectiveness model without compensation for natural convection enhancement effects.

Heat Exchanger	Collector Area (m^2)	Mass Flow Kg/Hr	M	F
Finned Spiral	3.0	300.0	1.8	0.3583
	3.0	300.0	1.0	0.3564
	6.5	300.0	1.8	0.5976
	6.5	300.0	1.0	0.5918
	10.0	600.0	1.8	0.7258
	10.0	600.0	1.0	0.7191
Smooth Coil	2.0	25.0	1.3	0.2415
	2.0	25.0	1.0	0.2412
	6.0	43.2	1.3	0.5049
	6.0	43.2	1.0	0.5039
	10.0	720.0	1.3	0.7280
	10.0	720.0	1.0	0.7250

Table 4. Yearly Simulation Results For Madison Solar DHW System

Heat Exchanger	Collector Area (m^2)	Mass Flow Kg/Hr	M	F
Single Wall Bayonet	2.0	14.4	1.35	0.2128
	2.0	14.4	1.0	0.2122
	6.0	250.0	1.35	0.5669
	6.0	250.0	1.0	0.5635
	10.0	720.0	1.35	0.7232
	10.0	720.0	1.0	0.7191
Double Wall Bayonet	2.0	144.0	1.7	0.2579
	2.0	144.0	1.0	0.2565
	6.0	432.0	1.7	0.5563
	6.0	432.0	1.0	0.5501
	10.0	72.0	1.7	0.6388
	10.0	72.0	1.0	0.6334

Table 5. Yearly Simulation Results For Madison Solar DHW System

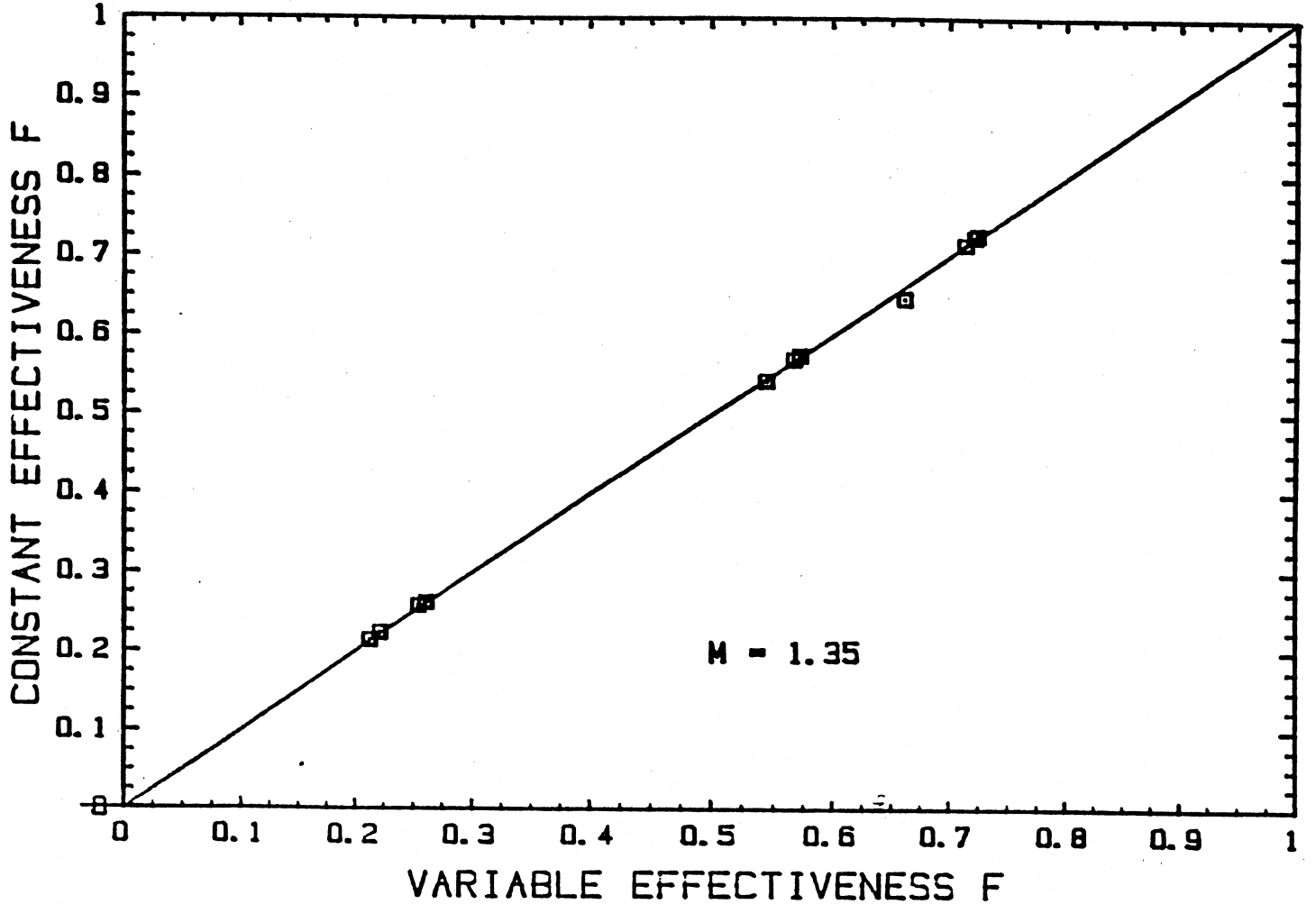

Figure 10. Comparison of Yearly Solar Fractions for Constant and Variable ε Simulations; Single Wall Bayonet Heat Exchanger, M=1.35.

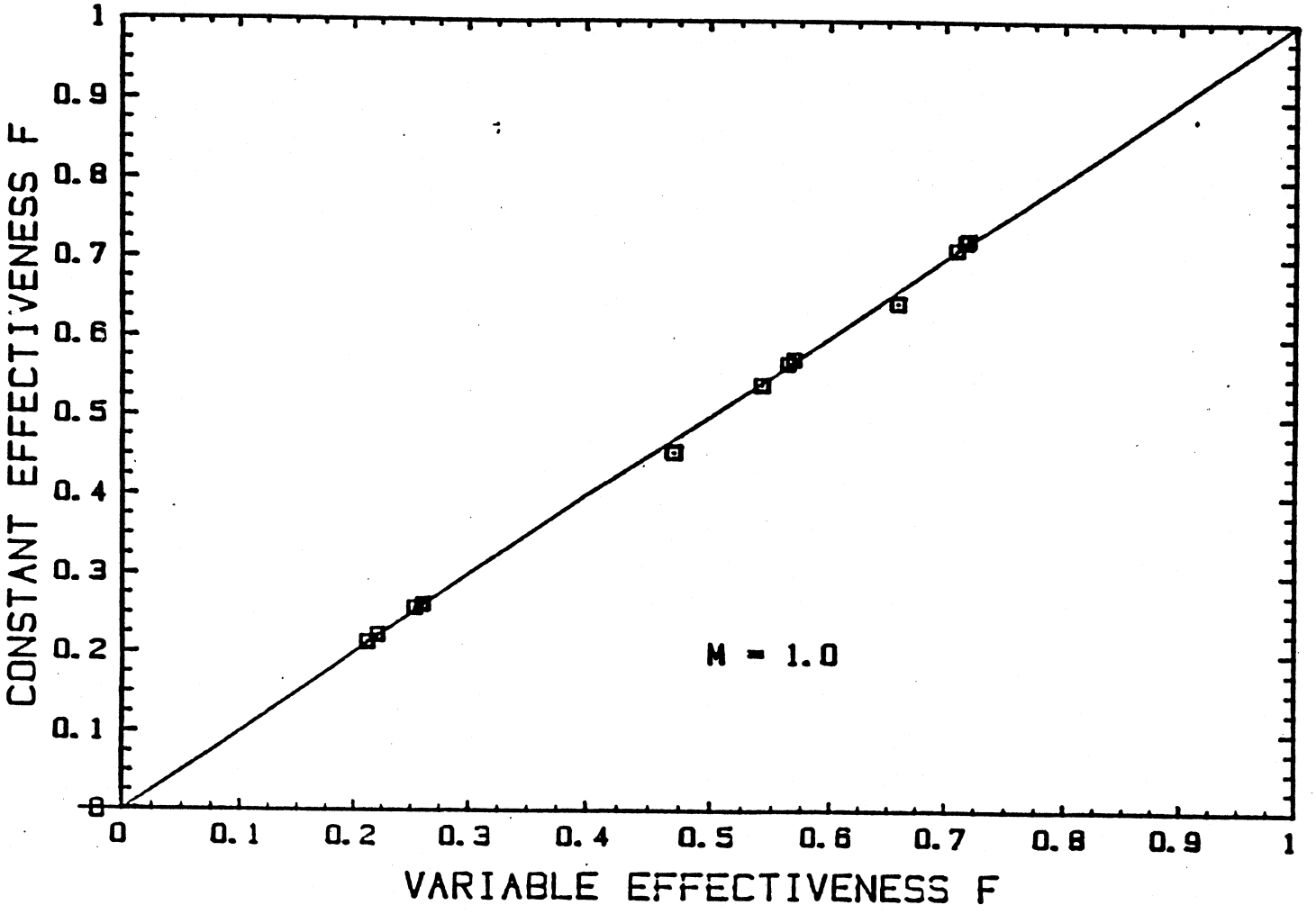

Figure 11. Comparison of Yearly Solar Fractions for Constant and Variable ε Simulations; Single Wall Bayonet Heat Exchanger, M=1.0.

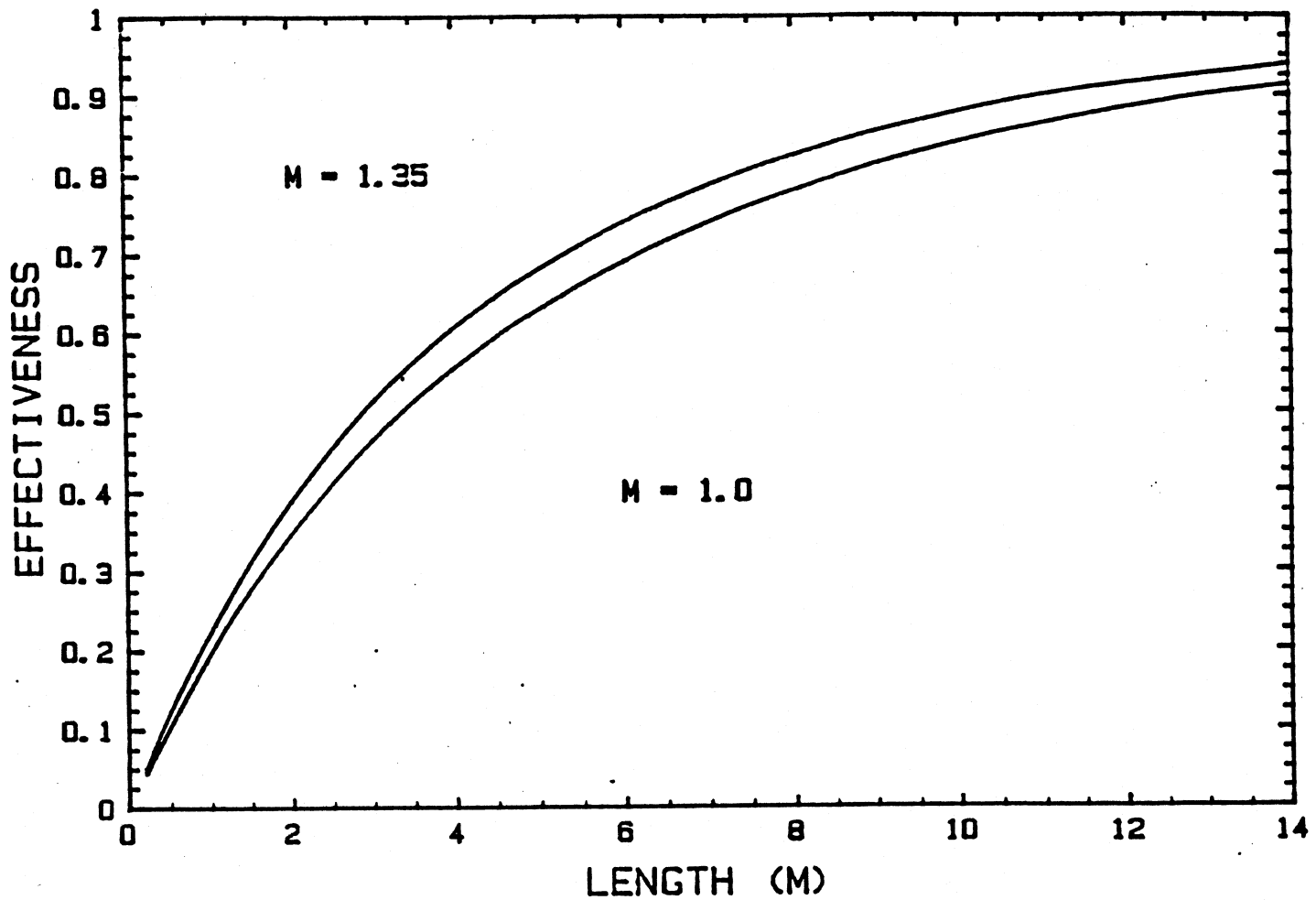

Figure 12. Estimated effectiveness vs. heat exchanger size, two values for M. Single wall bayonet heat exchanger, mass flow 324 kg/hour.

4.0 Discussion

This chapter contains a discussion of the results presented in Chapter 3. The section divisions in the chapter delineate the discussion along the lines of the major topics covered in the thesis. Section 1 is a comparison of the model performance with the experimental data generated by Farrington. Section 2 deals with the concept of enhancement of natural convection over immersed heat exchangers. Section 3 provides some guidelines for using the model.

4.1 Model vs. Experiment

Figures 5,6 and 7 in Chapter 3 provide an example of the dynamics of the experiments carried out by Farrington on each of the heat exchangers. The test run of the finned spiral heat exchanger was typical of all test runs, and provides an example for a discussion of the performance of the model.

Figure 6 demonstrates the effects of the lack of closure on the energy balance discussed in Chapter 3. The error in tank temperature is cumulative and attains a maximum of 3 C at the end of the simulation. The energy balance problem here is relatively insignificant for two reasons. First of all, the heat flow over the second half of the test,

where the error in tank temperature is greatest, is a small portion of the total heat flow, most of which occurs at the high temperature differences early in the test as seen in figure 5. Also, the error is small compared with the original temperature difference across the heat exchanger. The errors in the experimental data energy balance are not large enough to preclude the use of the data when checking the performance of the model.

Figure 8 is significant in that it demonstrates the importance of an accurate natural convection enhancement factor M. The effect of M in the Morgan correlation is constant along the entire length of the tube, and thus is an average natural convection factor for the tube. The resulting heat flow calculation is corrected only for high temperature differences, however. It is noted that while the selection of a single M for each heat exchanger provided good predictions of heat flow at each of three flow rates, the errors in simulated heat flow were not the same for each flow rate. For instance, the standard deviation in table 2 for the BENCHMARK simulation of the finned spiral heat exchanger shows that the error in simulated heat flow decreases with decreasing flow rates. This means that the value of M has a different effect on predicted heat flow at different flow rates. An individual value of M for each heat exchanger at each flow rate would provide better prediction of heat flow. The fact a single value of M provides close predictions of heat flow at three different flow rates

for one heat exchanger, though, means that the factor M, and thus the natural convection enhancement, is a weak function of the flow rate in the range of flow rates tested.

Figure 7 provides a good example of why the constant effectiveness model works. The simulated effectiveness is relatively constant for the simulation of the finned spiral heat exchanger test at a flowrate of 15 liters per minute, and this curve is characteristic of the effectivenesses in each of the simulated tests. The experimental effectiveness declines with time but this due to the lower experimental tank temperature. As has been demonstrated in figure 5 the heat flow in this example was predicted fairly accurately by the simulation. If the simulated effectiveness is relatively constant, then a constant effectiveness simulation may also be valid. Also, the relatively constant simulated effectiveness means that the temperature difference across the heat exchanger does not have a significant effect on the effectiveness. This is important when deviations from the fully mixed tank condition are examined. Cold layers of water may settle near or below the heat exchanger during a load draw, and this condition is ignored by the model. The calculated effectiveness will not be adversely affected, however, since it is insensitive to temperature differences.

Tables 2 and 3 contain the results of the statistical analysis. The standard deviation of the experimental heat flow about the fifth order curve fit to the heat

flow is shown in the first column of table 2 for each of the heat exchanger tests by Farrington. This standard deviation shows that the experimental noise is significant, and is generally higher at higher heat flows. The small bias error for the experimental heat flow data, shown in column 2 for each test run, means that the fifth order curve fit to the experimental heat flow data was good.

A comparison of the three simulation programs with the experimental data shows that the error in simulated heat flow is greater than the experimental noise. This can be seen in the columns of the standard deviation of simulated heat flow for each of the programs, the BENCHMARK program in column 3 of table 2, the SIMPLE program in column 1 of table 3 and the CONSTE program in column 3 of table 2. The standard deviation for the BENCHMARK and SIMPLE simulated heat flows are significantly higher than the standard deviation of the experimental heat flow in each test. The error in simulated heat flow for all three programs is significant, but as a percentage of total heat flow it is relatively small, and this can be seen in figure 5 which is a plot of simulated versus experimental heat flow for the finned spiral heat exchanger test at a 15 l/min flow rate.

The statistical errors for the BENCHMARK and SIMPLE simulations are nearly equivalent, and this can be seen by comparing the standard deviations in column 3 of table 2 and column 1 of table 3 for each test run. This result means that

the calculation of a UA from the average of UA values at the inlet and outlet of the heat exchanger is a good approximation to the changing UA along the length of the heat exchanger. The UA does not change enough along the length of the tube to alter the heat flow significantly.

The constant effectiveness algorithm CONSTE, in which the effectiveness is evaluated at the initial conditions (normally a 70 C inlet temperature and a 20 C bulk storage temperature) and is used for the rest of the simulation, provided some erratic results which belie the inherent inaccuracy in using a constant effectiveness assumption. The standard deviation of the predicted heat flow in these simulations was greater than the BENCHMARK standard deviation in some cases and less in others. The bias error did not follow a pattern either, sometimes negative, other times positive, which indicates that the errors in predicted heat flow were sometimes high and other times low. These results reinforce the idea that a constant effectiveness algorithm, while providing useful results, has errors which are unpredictable. The simplification of a constant effectiveness algorithm may sometimes be necessary, but there is a corresponding loss in accuracy.

4.2 Natural Convection Enhancement

Table 1 contains the enhancement factors found for each of the eight heat exchangers tested by Farrington and Feiereisen. The first four heat exchangers were tested by Feiereisen, two of which showed an enhanced heat transfer and two that showed a degradation of heat transfer when compared to heat transfer from an infinite tube in an infinite medium. The estimation of the M factors for the four heat exchangers was difficult, and this can be seen in the range of enhancement factors observed by Feiereisen.

First of all, heat exchanger configuration 1 is a single horizontal multi pass smooth tube and its enhancement factor is less than 1.0, which means the heat transfer from this coil is less than that from an infinite cylinder in an infinite medium. Heat exchanger configuration 4 is a series combination of two type 1 coils, yet its enhancement factor is 1.15, which means some enhancement of the natural convection heat transfer is occuring. What the effect the addition of a second coil had on the first coil is not possible to deduce.

The horizontal single pass smooth tube coil, coil 3, is shaped closest to the smooth infinite tube in an infinite medium. The heat exchanger is a single U-shaped tube and is horizontally positioned with the entire length of the tube in the same plane, thus there are no thermal effects from either above or below. The factor M, however, is the highest of the

group of heat exchangers from Feiereisen, which may lead to the conclusion that the most important enhancement of heat exchange results from the heat exchanger being placed in an enclosure.

The ranges observed by Feiereisen in the value of M demonstrate the difficulty in finding an accurate measurement of the natural convection heat transfer. Feiereisen made a great number of observations of the Nusselt number as a function of the Raleigh number for each heat exchanger and the range found for the value of M is attributed to the uncertainty of temperature measurements. Two series of observations of the Nusselt Rayleigh correlation for the horizontal, multi-pass, smooth tube coil (type 4) conducted 8 months apart verified the repeatability of these results. The final value of M for each of the four heat exchangers was found near the midpoint of the observations of M.

The heat exchangers tested by Farrington, heat exchangers 5-8, all showed some enhancement in natural convection. Only one value of M was found for each heat exchanger which was applicable for three tests at different flow rates. A limited amount of tests were run, and none of the test runs were repeated, so it was possible to find only one value of M for each test run, and the repeatability of this result is only possible if more test runs are completed for the four heat exchangers. Additional tests may result in a range of the M factor for each of the four heat exchangers investigated by Farrington similar to the ranges of M found by Feiereisen.

An explanation of the source of the value of M for the four heat exchangers tested by Farrington is just as difficult as it was for the tests run by Feiereisen. First, the two bayonet heat exchangers have geometries and overall dimensions which are similar, yet the values of the enhancement factors for the two are very different. The factor for the single wall bayonet is much lower than the factor for the double wall bayonet heat exchanger. The smooth coil heat exchanger is shaped like a cylinder of wrapped tubing where the tube lengths are in contact with each other, yet there is greater heat transfer from this coil than there is from an idealized tube, as the enhancement factor is greater than 1.0. The finned spiral heat exchanger is a geometry with the least amount of contact between different lengths of tubing, and the enhancement factor is very high compared to the other heat exchangers. This seems to suggest again, as the results for heat exchanger 3 did, that the enclosure accounts for a good deal of the enhancement of the natural convection heat exchange.

As was stated in Chapter 2 the geometries of the heat exchangers are unique and not usually held to close dimensional tolerances. The natural convection heat transfer is sensitive to changes in geometry as well as the enclosing walls of the storage tank and possibly other factors as well. The dimensional tolerances of the heat exchanger construction adds complication to the physical reasoning behind the value of M.

4.3 Heat Exchanger Design Guidelines

Some guidelines can be drawn for the use of this model when simulating capability is at a minimum. A simplification in the simulation algorithm which would allow a hand calculation comparison of different heat exchangers is the selection of a constant effectiveness. This method of calculation has already been explored with the use of the program CONSTE and the possible errors resulting from the simplification have been discussed. Two competing heat exchanger designs can be compared by calculating a constant effectiveness for each using the model developed in this thesis. A hand calculation of a heat exchanger effectiveness can be done using the algorithm outlined for the CONSTE program. A listing of the CONSTE program is located in appendix C. A sample hand calculation can be found in appendix E.

The calculations begin with the selection of a difference between the heat exchanger inlet temperature and the storage temperature. The CONSTE program used the initial conditions dictated by the experimental data supplied by Farrington and calculated an effectiveness at these conditions. The majority of the experiments conducted by Farrington began with an inlet temperature of 70 C and a tank temperature or 20

C. This temperature difference is suitable for a hand calculation of effectiveness, and the errors in the resulting prediction of heat transfer would be equivalent to those found using the CONSTE program. Starting with the thermal conditions an effectiveness can be calculated by finding an average UA for the entire heat exchanger as is done in CONSTE. There is an amount of iterative calculation due to the variability of water properties. The water properties do vary with temperature and some, like the Prandtl number, vary considerably. The water property values used in the hand calculation of effectiveness can be found using the water property correlations presented in appendix E.

One more problem with this type of hand calculation for a new heat exchanger is the selection of M. M, as has been shown, is impossible to determine analytically, and thus presents some difficulty. It has been shown in Chapter 3, tables 4 and 5, however, that the collector area penalty associated with the heat exchangers tested by Farrington at standard flow rates is small enough that the inclusion of M in the exterior heat transfer coefficient does not significantly affect the yearly performance of a solar domestic hot water system. This conclusion is true for heat exchanger flow rate combinations which result in a collector area penalty less than 10%. Smaller heat exchangers or low flow rates may result in greater system perfomance penalties, and an accurate estimation

of the natural convection heat transfer would then have more of an effect on the yearly solar fraction.

Figures 10 and 11 demonstrate an additional simplification. The estimation of a constant effectiveness for the heat exchangers tested results in yearly simulation results which are equivalent to those found with a variable effectiveness model. Again, this is due to the low collector area penalty associated with the heat exchanger flow rate combinations tested by Farrington. Errors that result from an assumption of constant effectiveness do not affect the collector area penalty significantly for systems with low collector area penalties to begin with.

5.0 Conclusions

A number of conclusions can be drawn from this study regarding the design and simulation of immersed, supply side heat exchangers.

First of all, the form of the model developed in this thesis is useful for predicting the heat flow from an immersed heat exchanger given some thermal conditions. The model equations were derived from basic principles and well known correlations for convection heat transfer. The characterization of the enhancement of natural convection heat transfer with a multiplicative constant M for the exterior heat transfer coefficient was the best possible solution to a problem which has not been analytically defined in the literature. The three programs derived from the model equations, BENCHMARK, SIMPLE and CONSTE, provide the basic coding for any type of simulations, including TRNSYS simulations. The SIMPLE algorithm provides a constant UA, variable effectiveness model which is as accurate in predicting heat flow as the BENCHMARK model which utilizes a variable UA to calculate the time dependent effectiveness. The simplification of the constant UA reduces the amount of calculations significantly.

The difficulty in defining and determining M for a heat exchanger configuration brings up a second result of this work, the need for more experimental analysis of natural con-

vection in tube banks and especially with immersed heat exchanger configurations. The major drawback in this model is the use of a constant which can only be determined experimentally. An analytical calculation of the enhancement of natural convection from immersed heat exchangers would greatly increase the capability to design an immersed heat exchanger and simulate its performance accurately without constructing a prototype.

The energy balance problem found in the heat exchanger test data provided by Farrington, which was discussed in Chapter 3, prevents any positive conclusions about the accuracy of the model or the values of M found for each of the four heat exchagers tested. A follow up study for the four heat exchangers in which the heat flow to the tank is accurately measured would be necessary for the conclusive verification of the model performance.

A final result of the thesis is the usefulness the model presents to heat exchanger designers. As has been stated, the small collector area penalties associated with well designed immersed heat exchangers means that the inclusion of M in the exterior heat transfer coefficient does not significantly affect the solar fraction in a year long simulation of a solar heating system. The small collector area penalty also allows the assumption of constant effectiveness in the calculation of yearly performance, as the errors associated with the constant effectiveness translate into very small

errors in the collector area penalty. A solar system designer, then, is able to design a heat exchanger without knowledge of the natural convection effects and with the assumption of constant effectiveness and expect acceptable yearly performance estimates. Heat exchager flow rate combinations which have a high collector area penalty do not fall within the range of these assumptions, however.

Appendix A

Listing of BENCHMARK program

```
      PROGRAM BENCHMARK
C
C THIS PROGRAM SIMULATES A HOT WATER TANK WITH AN INTERNAL
C SUPPLY SIDE HEAT EXCHANGER USING A FINITE DIFFERENCE
C METHOD TO CALCULATE THE ENERGY TRANSFER. THE HEAT EXHANGER
C MUST BE SMALL IN OVERALL DIMENSIONS RELATIVE TO THE SIZE OF
C THE TANK CAVITY AND BE BOTTOM MOUNTED IN ORDER TO INDUCE
C FULLY MIXED TANK CONDITIONS.
C
C VARIABLE AND ABBREVIATION DICTIONARY
C
C   AC       - AREA OF CONTACT RESISTANCE (M2)
C   AI       - INTERIOR AREA OF A LENGTH DELX OF HX TUBE (M2)
C              OR X-SECT AREA INSIDE TUBE IN SUBROUTINE INSIDE
C   AO       - EXTERIOR HEAT TRANSFER AREA FOR A LENGTH DELX OF
C              HX TUBE (M2)
C   AR       - AREA OF HEAT EXCHANGER WALL RESISTANCE; EQUAL TO
C              AN AVERAGE OF INTERIOR AND EXTERIOR AREAS (M2)
C   C        - EXTERIOR HEAT TRANSFER COEFFICIENT MULTIPLICATIVE
C              CONSTANT
C   CD       - CONTACT DIAMETER FOR DOUBLE WALL HX (M)
C   CK       - THERMAL CONDUCTIVITY OF PURE COPPER (W/M-K)
C   COEF     - VARIABLE REPRESENTING AN AMALGAMATED NATURAL
C              CONVECTION BOUYANCY COEFFICIENT (1/M3-K):
C                    COEF = (RHO**2)*BETA*CP*G/(MU*K)
C   CONST    - ARBITRARY CONSTANT
C   COR(21)  - THIS IS AN ARRAY CONTAINING THE LIQUID PROPERTY
C              CORRELATION COEFFICIENTS, AND IT IS INITIALIZED
C              IN SUBROUTINE CORREL
C   CP       - SPECIFIC HEAT (J/KG-K)
C   D        - DUMMY INTEGER VARIABLE
C   DA       - EXTERIOR HEAT TRANSFER AREA OF SINGLE SECTION OF
TUBE
C              LENGTH DELX IN SUBROUTINE SIMULATE (M2)
C   DELQ     - HEAT TRANSFER FROM A SINGLE SECTION OF TUBE
LENGTH
C              IN SUBROUTINE SIMULATE
C   DELT     - TI-TS  (K) AND TREF-TS IN SUBROUTINE SIMULATE (K)
C   DELTIME  - TIME STEP FOR THE SIMULATION (MIN)
C   DELX     - LENGTH OF TUBE SECTION IN SUBROUTINE SIMULATE (M)
C   DIFF     - REPRESENTS A NUMERICAL DIFFERENCE OF TWO COMPARED
NUMBERS(REAL)
C   EFF      - HX EFFECTIVENESS (DECIMAL)
C   EFFNTU   - EFFECTIVENESS CALCULATED AS 1.0-EXP(-NTU)
C   ETA      - FIN EFFICIENCY (DECIMAL)
```

```
C   F        - FACTOR IN PETUKHOV CORRELATION
C   FINA     - FRACTION OF HEAT TRANSFER AREA DUE TO FINS
(DECIMAL)
C   HC       - CONTACT COEFFICIENT FOR DOUBLE WALL HX (W/M2-K)
C   HI       - INTERIOR FORCED CONVECTIVE HEAT TRANSFER COEF-
FICIENT (W/M2-K)
C   HIGH     - UPPER LIMIT FOR RAYLEIGH NUMBER IN MORGAN COR-
RELATION
C              ALSO LIMIT FOR REYNOLDS NUMBER
C   HO       - EXTERIOR NATURAL CONVECTIVE HEAT TRANSFER COEF-
FICIENT (W/M2-K)
C   HX       - HEAT EXCHANGER
C   HTA      - EXTERNAL HEAT TRANSFER AREA, WHICH IS ADJUSTED
FOR
C              FIN EFFICIENCY BY USING THE FORMULA:
C                    HTA = HTA * ((1.0-FINA)+FINA*ETA)
C   ID       - HX INTERIOR DIAMETER (M)
C   J        - COUNTER (INT)
C   K        - THERMAL CONDUCTIVITY (W/M-K)
C   K1,K2    - CONSTANTS IN PETUKHOV CORRELATION
C   LEN      - HX TUBE LENGTH, UNBENT, (M)
C   LIM      - A NUMERICAL LIMIT (REAL)
C              ALSO DIVIDING VALUE FOR RAYLIEGH NUMBER BETWEEN
TWO FORMS OF
C              THE CURVE FIT IN MORGAN CORRELATION
C   LMTD     - LOG MEAN TEMPERATURE DIFFERENCE (K)
C   LOSS     - STORAGE TANK THERMAL LOSS (W/C)
C   LOW      - LOWER LIMIT FOR RAYLEIGH NUMBER IN MORGAN COR-
RELATION
C              ALSO LIMIT FOR REYNOLDS NUMBER
C   LW       - THICKNESS OF HEAT EXCHANGER WALL (M)
C   M        - NUMBER OF TIME STEPS IN SIMULATION (M)
C   MF       - HX HOT SIDE MASS FLOW (KG/S)
C   MFF(200) - ARRAY CONTAINING TIME VARIANT MASS FLOW DATA
(KG/S).
C   MID      - LIMITING VALUE OF RA IN MORGAN CORRELATION
C   MIDHI    - LIMITING VALUE OF RA IN MORGAN CORRELATION
C   MIDLO    - LIMITING VALUE OF RA IN MORGAN CORRELATION
C   MTANK    - MASS OF THE STORAGE TANK (KG)
C   MUBULK   - DYNAMIC VISCOSITY OF HEAT EXCHANGER FLUID (N-
S/M2)
C   MUWALL   - DYNAMIC VISCOSITY OF HEAT EXCHANGER FLUID AT
INTERIOR
C              WALL TEMPERATURE (N-S/M2)
C   NU       - KINEMATIC VISCOSITY (M2/S)
C   NUSIN    - INTERIOR FORCED CONVECTIVE NUSSELT NUMBER
C   NUSOUT   - EXTERIOR NATURAL CONVECTIVE NUSSELT NUMBER
C   OD       - HX TUBE OUTSIDE DIAMETER, DISCOUNTING FINS (M)
C   PI       - 3.1415927
C   POS      - POSITION COUNTER USED TO DENOTE DISTANCE FROM THE
```

```
C                STARTING END OF THE TUBE (M)
C   PR         - PRANDTL NUMBER
C   QA         - HEAT TRANSFER PER UNIT AREA (W/M2-K)
C   QLEN       - HEAT TRANSFER FROM ENTIRE HEAT EXCHANGER (WATTS)
C   R          - CALCULATED CONTACT RESISTANCE R=1.0/(AC*HC)
(K/W)
C   RA         - RAYLEIGH NUMBER
C   RE         - REYNOLDS NUMBER
C   RHO        - DENSITY (KG/M3)
C   SEE        - SPECIFIC TIME IN THE SIMULATION WHEN PARAMETER
DATA
C                IS RECORDED (MIN)
C   TI         - HX HOT WATER INLET TEMPERATURE (K)
C   TII(200)- ARRAY CONTAINING HX HOT SIDE INLET TEMPERATURES
C                FOR EACH TIME STEP (K)
C   TM         - PRESENT TIME (MIN)
C   TO         - TEMPERATURE ON HOT SIDE OF HX AT THE DOWNSTREAM
END OF
C                SINGLE SECTION DELX OF TUBE LENGTH (K)
C   TONEW      - RECALCULATED TO (K)
C   TREF       - (TX+TO)/2, OR THE MEDIAN TEMPERATURE IN A SINGLE
SECTION OF
C                TUBE LENGTH (K)
C   TS         - STORAGE TANK BULK TEMPERATURE (K)
C   TW         - HX TUBE WALL TEMPERATURE (K)
C   TWNEW      - RECALCULATED TW (K)
C   TX         - HX HOT SIDE OUTLET TEMPERATURE (K), OR EXIT
TEMPERATURE
C                FROM EACH SECTION OF HX IN SUBROUTINE SIMULATE
C   UA         - OVERALL HEAT TRANSFER COEFFICIENT AREA PRODUCT
(W/K)
C   UAI        - HEAT TRANSFER COEFFICIENT FOR HOT SIDE OF HX,
INCLUDING
C                CONTACT RESISTANCE (W/K)
C   UM         - MEAN FLUID VELOCITY ON HOT SIDE OF HX (M/S)
C
      REAL COR(21),TI,TS,LEN,MF,C,OD,ID,EFF,TII(200),MFF(200)
      REAL COEF,NU,K,PR,CP,RHO,DELTIME,TM,QLEN,TX
      REAL DELT,UA,LMTD,HTA,CD,HC,LOSS,MTANK
      INTEGER J,M,D
      CALL CORREL(COR)
C
C INPUT FILES
C
      OPEN(50,FILE='FINNED.DAT',READ ONLY,STATUS='OLD')
      OPEN(57,FILE='[MATES.ARCHIVE]FINNED15.ORIG',READ ONLY,
     + STATUS='OLD')
C
C OUTPUT FILES
C
```

```
      OPEN(60,FILE='PARAM.DAT',STATUS='NEW')
C      WRITE(60,*)'TIME(MIN)  HXI(C)  TS(C)  Q(W)  UA(W/C)
EFF'
      OPEN(70,FILE='RAYL.DAT',STATUS='NEW')
C
C PARAMETER INPUT
C
      READ(57,*)M,DELTIME
C      WRITE(60,61)M,DELTIME
C61    FORMAT(1X,I6,F6.1)
      WRITE(6,*)'M=',M,'DELTIME=',DELTIME
      DO 25,J=1,M
         READ(57,*)TM,D,TII(J),TS,TS,MFF(J),QLEN,UA,TS,TS
         TII(J)=TII(J)+273.15
25    CONTINUE
      CALL PARAM(TS,LEN,C,OD,ID,COR,HTA,CD,HC)
C
      CALL PROP(TS,COEF,COR,NU,K,PR,CP,RHO)
C
      MTANK=0.409*RHO
C
      LOSS=1.6
C
C THIS LOOP SIMULATES THE TANK-HEAT EXCHANGER OVER TIME,
ADJUSTING THE
C TANK TEMPERATURE EVERY DELTIME MINUTES.
C THE HEAT FLOW PORTION HERE WAS HAND CHECKED GOOD-SPRING BREAK
C
C INITIALIZE TIME: TIME AND HEAT FLOW CALCULATIONS AT ONE TIME
C REPRESENT THE CONDITIONS FOR THE TIME PERIOD FOLLOWING UNTIL
C ANOTHER CALCULATION IS MADE
      TM=0.0
C
      DO 20, J=1,M
C SET TIME AND INLET TEMPERATURE
         TI=TII(J)
         MF=MFF(J)
C CALCULATE MASS FLOW AT INLET TEMPERATURE
         CALL PROP(TI,COEF,COR,NU,K,PR,CP,RHO)
         MF=MF*(RHO/(60.0*1000.0))
C CHECK FOR ZERO MASS FLOW
         IF(MF.EQ.0.0)THEN
            QLEN=0.0
            EFF=0.0
            GOTO 40
         ENDIF
C SIMULATE
         CALL
SIMULATE(EFF,TI,TS,LEN,MF,OD,ID,COR,QLEN,TM,HTA,CD,HC,C)
40       CONTINUE
```

```
C CALCULATE SYSTEM PARAMETERS
         CALL PROP(TS,COEF,COR,NU,K,PR,CP,RHO)
         DELT=TI-TS
         TX=TI-EFF*(TI-TS)
C         LMTD=(TI-TX)/LOG((TI-TS)/(TX-TS))
C         UA=QLEN/LMTD
         UA=999.0
C
C CONVERT TEMPERATURES AND OUTPUT RESULTS TO FILE
C
         TS=TS-273.15
         TI=TI-273.15
         TX=TX-273.15
         WRITE(60,90)TM,TI,TX,TS,QLEN,UA,EFF
C RETURN TEMPERATURES TO KELVIN
         TS=TS+273.15
         TI=TI+273.15
         TX=TX+273.15
C STEP TIME
         TM=TM+DELTIME
C STEP TANK TEMPERATURE
         TS=TS+QLEN*DELTIME*60.0/(MTANK*CP)
         TS=TS-LOSS*(TS-293.15)*DELTIME*60.0/(MTANK*CP)
C SET MF BACK TO LITERS/MIN
         CALL PROP(TI,COEF,COR,NU,K,PR,CP,RHO)
         MF=MF/(RHO/(60.0*1000.0))
20     CONTINUE
C
90     FORMAT(1X,F10.1,3F8.2,2F10.2,F8.3)
       STOP
       END
C
C
       SUBROUTINE
SIMULATE(EFF,TI,TS,LEN,MF,OD,ID,COR,QLEN,TM,HTA,CD,HC,
     +C)
C
C THIS SUBROUTINE DIVIDES THE HEAT EXCHANGER INTO 30 SECTIONS
AND CALCULATES
C THE HEAT FLOW AND INSIDE TEMPERATURE DROP FOR EACH SECTION.
C
C HAND CHECK GOOD-SPRING BREAK
C
       REAL EFF,TI,TS,LEN,MF,OD,ID,COR(21)
       REAL PI,TX,DELX,HI,TW,DA,QA
       REAL COEF,NU,K,PR,CP,RHO,QLEN
       REAL NUSOUT,HO,TM,RA,POS,SEE,CD,HC
       REAL EFFNTU,TREF,DELQ,DELT,HTA,C
       REAL AI,AO,AC,R,UA
       INTEGER I
```

```
C PARAMETER INITIALIZATION
      PI=3.1415927
      SEE=5.0
      DELX=LEN/30.0
      AI=PI*ID*DELX
      AO=HTA*DELX/LEN
      AC=PI*CD*DELX
      IF(AC.EQ.0.0)THEN
         R=0.0
      ELSE
         R=1.0/(HC*AC)
      ENDIF
      TX=TI
      QLEN=0.0
      DA=HTA*DELX/LEN
C LOOP CALCULATES AND SUMS HEAT FLOW FOR EACH OF 30 SECTIONS
      DO 100,I=1,30
C TWALL CALCULATES WALL TEMPERATURE FOR SECTION
         CALL
TWALL(TX,TS,TW,OD,COR,TI,DELX,LEN,MF,ID,TO,HTA,CD,HC,C)
C GIVEN TW, HO IS CALCULATED
         CALL OUTSIDE(TS,TW,OD,COR,NUSOUT,HO,RA,C)
C GIVEN TW AND TO, HI IS CALCULATED FROM THE MEDIAN SECTION
TEMPERATURE
         TREF=(TX+TO)/2.0
         CALL INSIDE(TREF,HI,MF,ID,COR,TW)
C HEAT TRANSFER PARAMETERS ARE CALCULATED
         UA=1.0/(1.0/(HO*AO)+1.0/(HI*AI)+R)
         QA=HO*(TW-TS)
         DELQ=QA*DA
         DELT=TREF-TS
C PARAMETERS OUTPUT TO FILE AT TIME SEE
         IF(TM.EQ.SEE)THEN
            POS=(I-1)*DELX+(DELX/2.0)
            WRITE(70,71)POS,HO,HI,UA,TREF,TS,DELQ
         ENDIF
C HOT SIDE TEMPERATURE INCREMENTED ALONG LENGTH
         CALL PROP(TREF,COEF,COR,NU,K,PR,CP,RHO)
         TX=TX-(DA*QA/(MF*CP))
         QLEN=QLEN+DA*QA
C
100   CONTINUE
C
71    FORMAT(1X,F7.2,2F9.1,F8.2,3F8.1)
C EFFECTIVENESS CALCULATED
      EFF=(TI-TX)/(TI-TS)
      RETURN
      END
C
C
```

```
      SUBROUTINE PROP(T,COEF,COR,NU,K,PR,CP,RHO)
      REAL T,COR(21),COEF,NU,K,PR,RHO
C THIS SUBROUTINE CALCULATES VALUES FOR LISTED WATER
C PROPERTIES GIVEN A WATER TEMPERATURE
C HAND CHECK GOOD-SPRING BREAK
      PR=COR(1)*EXP(COR(2)/T)+COR(3)
      COEF=COR(4)+COR(5)*T+COR(6)*(T**2)
      COEF=COEF*(1.0E9)
      NU=COR(7)*EXP(COR(8)/T)+COR(9)
      NU=NU/1.0E6
      K=COR(10)+COR(11)*T+COR(12)*(T**2)
      CP=COR(13)+COR(14)*T+COR(15)*(T**2)
      CP=CP+COR(16)*(T**3)+COR(17)*(T**4)
      RHO=COR(18)+COR(19)*T+COR(20)*(T**2)
      RHO=RHO+COR(21)*(T**3)
      RETURN
      END
C
C
      SUBROUTINE
TWALL(TX,TS,TW,OD,COR,TI,DELX,LEN,MF,ID,TO,HTA,CD,HC,C)
C
C THIS SUBROUTINE BALANCES FOUR HEAT TRANSFER RATE EQUATIONS IN
ORDER TO
C CALCULATE TW AND TO FOR EACH SECTION OF HX TUBE LENGTH. THE
FOUR EQUATIONS
C ARE:
C           Q = HO*AO*(TW-TS) = UAI*(TREF-TW)
C AND
C           Q = MF*CP*(TX-TO) = UA*(TREF-TS)
C
C A SUCCESSIVE SUBSTITUTION METHOD IS USED TO ARRIVE AT THE TWO
UNKNOWN
C QUANTITIES TO AND TW. THE HEAT TRANSFER IS THEN CALCULATED
FROM THESE
C PARAMETERS
C
      REAL TX,TS,TW,OD,COR(21),TI,DELX,LEN,MF,ID
      REAL NUSOUT,HO,HI,DIFF,RA,AI,AO,TREF,LIM,TO
      REAL TWNEW,TONEW,PI,UA,R,UAI,AC
      REAL COEF,NU,K,PR,CP,RHO,HTA,CD,HC,C
C INITIALIZATION
      PI=3.1415927
      LIM=0.0001
      AI=PI*ID*DELX
      AO=HTA*DELX/LEN
      AC=PI*CD*DELX
      IF(AC.EQ.0.0)THEN
         R=0.0
      ELSE
```

```
         R=1.0/(HC*AC)
      ENDIF
C INTIAL GUESSES
      TO=TX-(TI-TS)/(LEN/DELX)
      TW=(8.0/9.0)*((TX+TO)/2.0-TS)+TS
C BEGINNING OF SUCCESSIVE SUBSTITUTION LOOP
300   CONTINUE
C FIRST LOOP CALCULATES NEW TW
         CALL OUTSIDE(TS,TW,OD,COR,NUSOUT,HO,RA,C)
         TREF=(TO+TX)/2.0
         CALL INSIDE(TREF,HI,MF,ID,COR,TW)
         UAI=1.0/(1.0/(HI*AI)+R)
         TWNEW=(UAI*(TX+TO)/2.0+HO*AO*TS)/(UAI+HO*AO)
C CHECK
         DIFF=ABS(TWNEW-TW)
         IF(DIFF.GT.LIM)THEN
            TW=TWNEW
            GOTO 300
         ENDIF
C END OF FIRST LOOP
310   CONTINUE
C SECOND LOOP CALCULATES NEW TO
         UA=1.0/(1.0/(HO*AO)+1.0/(HI*AI)+R)
         CALL PROP(TREF,COEF,COR,NU,K,PR,CP,RHO)
         TONEW=(MF*CP*TX-UA*TX/2.0+UA*TS)/(MF*CP+(UA/2.0))
C CHECK
         DIFF=ABS(TONEW-TO)
         IF(DIFF.GT.LIM)THEN
            TO=TONEW
            GOTO 300
         ENDIF
320   CONTINUE
C END OF SECOND LOOP
      RETURN
      END
C
C
      SUBROUTINE INSIDE(TREF,HI,MF,ID,COR,TW)
C THIS SUBROUTINE CALCULATES THE INSIDE FORCED CONVECTIVE
C HEAT TRANSFER COEFFICIENT USING THE PETUKHOV EQUATION
C HAND CHECK GOOD-SPRING BREAK
      REAL TREF,HI,MF,ID,PI,AI,COR(21),TW
      REAL COEF,NU,K,PR,CP,RHO
      REAL RE,UM,F,K1,K2,NUSIN,CONST
      REAL HIGH,LOW,MUBULK,MUWALL,MID
      PI=3.1415927
      HIGH=5.0E06
      MID=1.0E04
      LOW=2300.0
      AI=PI*((ID/2.0)**2)
```

```
      CALL PROP(TW,COEF,COR,NU,K,PR,CP,RHO)
      MUWALL=RHO*NU
      CALL PROP(TREF,COEF,COR,NU,K,PR,CP,RHO)
      MUBULK=RHO*NU
      UM=MF/(RHO*AI)
      RE=UM*ID/NU
      IF(RE.GT.HIGH)THEN
         WRITE(6,*)'REYNOLDS OUT OF BOUNDS',RE,'TREF=',TREF
      ENDIF
      IF(RE.LE.LOW)THEN
         NUSIN=3.66
      ELSE
         IF(RE.GT.LOW.AND.RE.LT.MID)THEN
            F=1.0/((1.82*LOG10(MID)-1.64)**(2.0))
            NUSIN=(F/8.0)*MID*PR
            K1=1.0+3.4*F
            K2=11.7+1.8/(PR**0.333333)
            CONST=K1+K2*((F/8.0)**0.5)*((PR**0.66667)-1.0)
            NUSIN=NUSIN/CONST
            NUSIN=NUSIN*((MUBULK/MUWALL)**0.25)
            NUSIN=NUSIN-(NUSIN-3.66)*(10000.0-RE)/7700
         ELSE
            F=1.0/((1.82*LOG10(RE)-1.64)**(2.0))
            NUSIN=(F/8.0)*RE*PR
            K1=1.0+3.4*F
            K2=11.7+1.8/(PR**0.333333)
            CONST=K1+K2*((F/8.0)**0.5)*((PR**0.66667)-1.0)
            NUSIN=NUSIN/CONST
            NUSIN=NUSIN*((MUBULK/MUWALL)**0.25)
         ENDIF
      ENDIF
      HI=K*NUSIN/ID
      RETURN
      END
C
C
      SUBROUTINE OUTSIDE(TS,TW,OD,COR,NUSOUT,HO,RA,C)
C THIS SUBROUTINE CALCULATES THE OUTSIDE NATURAL CONVECTIVE
C HEAT TRANSFER COEFFICIENT USING THE MORGAN CORRELATION
C HAND CHECK GOOD-SPRING BREAK
      REAL TS,TW,OD,COR(21),NUSOUT,HO,PI,RA,TREF,C
      REAL COEF,NU,K,PR,CP,RHO,LOW,HIGH,MIDLO,MID,MIDHI
      HIGH=1.0E+12
      MIDHI=1.0E+07
      MID=1.0E+04
      MIDLO=1.0E+02
      LOW=1.0E-02
      PI=3.1415927
      TREF=(TW+TS)/2.0
      CALL PROP(TREF,COEF,COR,NU,K,PR,CP,RHO)
```

```
      RA=COEF*(OD**3)*ABS(TW-TS)
C THIS LOOP WARNS OF A RAYLEIGH NUMBER OUT OF THE BOUND
C OF THE MORGAN CORRELATION
C
C MORGAN CORRELATION
      IF(RA.LT.LOW)THEN
         WRITE(6,*)'RAYLEIGH NUMBER TOO LOW',RA
         WRITE(60,*)'RAYLEIGH NUMBER TOO LOW',RA
      ELSEIF(RA.GE.LOW.AND.RA.LT.MIDLO)THEN
         NUSOUT=1.02*(RA**0.148)
      ELSEIF(RA.GE.MIDLO.AND.RA.LT.MID)THEN
         NUSOUT=0.85*(RA**0.188)
      ELSEIF(RA.GE.MID.AND.RA.LT.MIDHI)THEN
         NUSOUT=0.48*(RA**0.25)
      ELSEIF(RA.GE.MIDHI.AND.RA.LE.HIGH)THEN
         NUSOUT=0.125*(RA**0.333)
      ELSEIF(RA.GT.HIGH)THEN
         WRITE(60,*)'RAYLIEGH TOO HIGH',RA
         WRITE(6,*)'RAYLIEGH TOO HIGH',RA
      ENDIF
C
      NUSOUT=C*NUSOUT
C
      HO=K*NUSOUT/OD
      RETURN
      END
C
C
      SUBROUTINE PARAM(TS,LEN,C,OD,ID,COR,HTA,CD,HC)
C
C THIS SUBROUTINE READS IN DATA FOR TANK TRIALS FROM FILE 50,
C THE UNITS READ IN ARE AS FOLLOWS:
C       TS - DEG C
C       LEN - METERS
C       C - REAL
C       OD,ID - MM
C       HTA - HEAT TRANSFER AREA (OUTSIDE) - M2
C       FINA - PERCENT % HEAT TRANSFER AREA DUE TO FINS (AS
DECIMAL)
C       ETA - FIN EFFICIENCY (AS DECIMAL)
C       CD - CONTACT DIAMETER (MM)
C       HC - CONTACT COEFFICIENT (W/M2-K)
C
C HAND CHECK GOOD
      REAL TS,LEN,C,OD,ID,HTA,FINA,ETA,HC,CD
      REAL COEF,COR(21),NU,K,PR,CP,RHO
      READ(50,*)TS,LEN,C,OD,ID,HC
      READ(50,*)HTA,FINA,ETA,CD
C OUTPUT PARAMETERS TO CHECK
      WRITE(6,*)'TS=',TS,'C'
```

```
      WRITE(6,*)'LEN=',LEN,'M   C=',C
      WRITE(6,*)'OD=',OD,'MM   ID=',ID,'MM'
      WRITE(6,*)'CONTACT COEFFICIENT=',HC,'W/M2-K'
      WRITE(6,*)'TOTAL OUTSIDE HEAT TRANSFER AREA =',HTA,'M2'
      WRITE(6,*)'FRACTION OF HT AREA DUE TO FINS=',FINA
      WRITE(6,*)'FIN EFFICIENCY=',ETA
      WRITE(6,*)'CONTACT DIAMETER=',CD,'MM'
C CONVERT PARAMETERS TO UNITS USED IN PROGRAM
      TS=TS+273.15
      OD=OD/1000.0
      ID=ID/1000.0
      CD=CD/1000.0
C ADJUST HEAT TRANSFER AREA TO ACCOUNT FOR FIN EFFICIENCY
      HTA=HTA*((1.0-FINA)+FINA*ETA)
      WRITE(6,*)'ADJUSTED HEAT TRANSFER AREA=',HTA
      RETURN
      END
C
C
      SUBROUTINE CORREL(COR)
C THIS SUBROUTINE INPUTS THE COEFFICIENTS USED IN THE PROPERTY
C CORRELATIONS
      REAL COR(21)
      COR(1)=0.7408843E-03
      COR(2)=0.2642356E+04
      COR(3)=0.8893757
      COR(4)=414.691
      COR(5)=-3.784647
      COR(6)=0.008245761
      COR(7)=0.2324911E-03
      COR(8)=0.2407664E+04
      COR(9)=0.1494501
      COR(10)=-0.4890243
      COR(11)=0.5895468E-02
      COR(12)=-0.7400855E-05
      COR(13)=0.3893872E+05
      COR(14)=-0.4150730E+03
      COR(15)=0.1859918E+01
      COR(16)=-0.3710142E-02
      COR(17)=0.2783111E-05
      COR(18)=271.0915
      COR(19)=6.420254
      COR(20)=-0.1772474E-01
      COR(21)=0.1461599E-04
      RETURN
      END
```

Appendix B

Listing of program SIMPLE

Note: subroutines PROP, INSIDE, OUTSIDE, PARAM, and CORREL are identical to the subroutines of the same name in program BENCHMARK, and will not be printed in this appendix.

```
      PROGRAM SIMPLE
C
C THIS IS THE SIMPLIFIED VERSION OF TANK WITH A SINGLE UA CAL-
CULATION
C FOR THE ENTIRE TUBE AT EACH TIME STEP.
C
      REAL COR(21),TI,TS,LEN,MF,C,OD,ID,EFF,TII(200),MFF(200)
      REAL COEF,NU,K,PR,CP,RHO,DELTIME,TM,QLEN,TX
      REAL DELT,UA,LMTD,HTA,CD,HC,LOSS,MTANK
      INTEGER J,M,D
      CALL CORREL(COR)
C
C INPUT FILES
C
      OPEN(50,FILE='FINNED.DAT',READ ONLY,STATUS='OLD')
      OPEN(57,FILE='[MATES.ARCHIVE]FINNED15.ORIG',READ ONLY,
     + STATUS='OLD')
C
C OUTPUT FILES
C
      OPEN(60,FILE='PARAM.DAT',STATUS='NEW')
C      WRITE(60,*)'TIME(MIN)  HXI(C)  TS(C)  Q(W)  UA(W/C)
EFF'
      OPEN(70,FILE='RAYL.DAT',STATUS='NEW')
C
C PARAMETER INPUT
C
      READ(57,*)M,DELTIME
C      WRITE(60,63)M,DELTIME
63    FORMAT(1X,I10,F8.2)
      WRITE(6,*)'M=',M,'DELTIME=',DELTIME
      DO 25,J=1,M
         READ(57,*)TM,D,TII(J),TS,TS,MFF(J),QLEN,UA,TS,TS
         TII(J)=TII(J)+273.15
25    CONTINUE
      CALL PARAM(TS,LEN,C,OD,ID,COR,HTA,CD,HC)
C
```

```
      CALL PROP(TS,COEF,COR,NU,K,PR,CP,RHO)
C
      MTANK=0.409*RHO
C THIS IS A TEST
C      MTANK=0.5*RHO
C
      LOSS=1.6
C
C THIS LOOP SIMULATES THE TANK-HEAT EXCHANGER OVER TIME,
ADJUSTING THE
C TANK TEMPERATURE EVERY DELTIME MINUTES.
C THE HEAT FLOW PORTION HERE WAS HAND CHECKED GOOD-SPRING BREAK
C
C INITIALIZE TIME: TIME AND HEAT FLOW CALCULATIONS AT ONE TIME
C REPRESENT THE CONDITIONS FOR THE TIME PERIOD FOLLOWING UNTIL
C ANOTHER CALCULATION IS MADE
C
      TM=0.0
C
      DO 20, J=1,M
C SET MASS FLOW AND INLET TEMPERATURE
         TI=TII(J)
         MF=MFF(J)
C CALCULATE MASS FLOW AT INLET TEMPERATURE
         CALL PROP(TI,COEF,COR,NU,K,PR,CP,RHO)
         MF=MF*(RHO/(60.0*1000.0))
C CHECK FOR ZERO MASS FLOW RATE
         IF(MF.EQ.0.0)THEN
            QLEN=0.0
            EFF=0.0
            GOTO 40
         ENDIF
C SIMULATE
         CALL
SIMULATE(EFF,TI,TS,LEN,MF,OD,ID,COR,QLEN,HTA,CD,HC,C,TM)
40       CONTINUE
C CALCULATE SYSTEM PARAMETERS
         CALL PROP(TS,COEF,COR,NU,K,PR,CP,RHO)
         DELT=TI-TS
         TX=TI-EFF*(TI-TS)
C         LMTD=(TI-TX)/LOG((TI-TS)/(TX-TS))
C         UA=QLEN/LMTD
         UA=999.0
C
C CONVERT TEMPERATURES AND OUTPUT RESULTS TO FILE
C
         TS=TS-273.15
         TI=TI-273.15
         TX=TX-273.15
         WRITE(60,90)TM,TI,TX,TS,QLEN,UA,EFF
```

```
C RETURN TEMPERATURES TO KELVIN
         TS=TS+273.15
         TI=TI+273.15
         TX=TX+273.15
C STEP TIME
         TM=TM+DELTIME
C STEP TANK TEMPERATURE
         TS=TS+QLEN*DELTIME*60.0/(MTANK*CP)
         TS=TS-LOSS*(TS-293.15)*DELTIME*60.0/(MTANK*CP)
C SET MF BACK TO LITERS/MIN
         CALL PROP(TI,COEF,COR,NU,K,PR,CP,RHO)
         MF=MF/(RHO/(60.0*1000.0))
20     CONTINUE
C
90     FORMAT(1X,F10.1,3F8.2,2F10.2,F8.3)
900    CONTINUE
       STOP
       END
C
C
       SUBROUTINE
SIMULATE(EFF,TI,TS,LEN,MF,OD,ID,COR,QLEN,HTA,CD,HC,C
     +,TM)
C
       REAL EFF,TI,TS,LEN,MF,OD,ID,COR(21),QLEN,HTA,CD,HC,C
       REAL COEF,NU,K,PR,CP,RHO
       REAL PI,TO,HI,TW,DELX,TREF,AI,AO,AC,R,LIM,DIFF
       REAL NUSOUT,HO,RA,NTU,UA,UA1,UA100,TONEW,LOW
       INTEGER I,ITER
C PARAMETER INITIALIZATION
       PI=3.1415927
       LOW=1.0E-04
       DELX=LEN/100.0
       AI=PI*ID*DELX
       AO=HTA*DELX/LEN
       AC=PI*CD*DELX
       IF(AC.EQ.0.0)THEN
          R=0.0
       ELSE
          R=1.0/(HC*AC)
       ENDIF
       QLEN=0.0
       CALL TWALL(TI,TS,TW,OD,COR,DELX,LEN,MF,ID,HTA,CD,HC,C)
       CALL OUTSIDE(TS,TW,OD,COR,NUSOUT,HO,RA,C)
       CALL INSIDE(TI,HI,MF,ID,COR,TW)
       UA1=1.0/(1.0/(HO*AO)+1.0/(HI*AI)+R)
       UA=100.0*UA1
       TO=TI
       ITER=0
100    CONTINUE
```

```
            ITER=ITER+1
            CALL TWALL(TO,TS,TW,OD,COR,DELX,LEN,MF,ID,HTA,CD,HC,C)
            CALL OUTSIDE(TS,TW,OD,COR,NUSOUT,HO,RA,C)
            CALL INSIDE(TO,HI,MF,ID,COR,TW)
            UA100=1.0/(1.0/(HO*AO)+1.0/(HI*AI)+R)
            UA=100.0*((UA1+UA100)/2.0)
            TREF=(TI+TO)/2.0
            CALL PROP(TREF,COEF,COR,NU,K,PR,CP,RHO)
            NTU=UA/(MF*CP)
            EFF=1.0-EXP(-NTU)
            TONEW=TI-EFF*(TI-TS)
            LIM=0.001*(TI-TO)
            IF(LIM.LT.LOW)THEN
               LIM=LOW
            ENDIF
            DIFF=ABS(TONEW-TO)
            IF(DIFF.GT.LIM)THEN
               TO=TONEW
               GOTO 100
            ENDIF
         CONTINUE
         QLEN=MF*CP*(TI-TO)
         RETURN
         END
C
C
         SUBROUTINE
TWALL(TX,TS,TW,OD,COR,DELX,LEN,MF,ID,HTA,CD,HC,C)
C
C THIS SUBROUTINE BALANCES TWO HEAT TRANSFER RATE EQUATIONS IN
ORDER TO
C CALCULATE TW FOR THE BEGINNING AND END OF THE TUBE, AS
SPECIFIED IN
C SUBROUTINE SIMULATE
C              Q = HO*AO*(TW-TS) = UAI*(TX-TW)
C A SUCCESSIVE SUBSTITUTION METHOD IS USED TO ARRIVE AT THE
UNKNOWN
C QUANTITY TW. THE HEAT TRANSFER IS THEN CALCULATED FROM THIS
PARAMETER
C
         REAL TX,TS,TW,OD,COR(21),DELX,LEN,MF,ID
         REAL NUSOUT,HO,HI,DIFF,RA,AI,AO,LIM
         REAL TWNEW,PI,UA,R,UAI,AC
         REAL COEF,NU,K,PR,CP,RHO,HTA,CD,HC,C
C INITIALIZATION
         PI=3.1415927
         LIM=0.0001
         AI=PI*ID*DELX
         AO=HTA*DELX/LEN
         AC=PI*CD*DELX
```

```
      IF(AC.EQ.0.0)THEN
         R=0.0
      ELSE
         R=1.0/(HC*AC)
      ENDIF
C INTIAL GUESS
      TW=(4.0/5.0)*(TX-TS)+TS
C BEGINNING OF SUCCESSIVE SUBSTITUTION LOOP
300   CONTINUE
C LOOP CALCULATES NEW TW
         CALL OUTSIDE(TS,TW,OD,COR,NUSOUT,HO,RA,C)
         CALL INSIDE(TX,HI,MF,ID,COR,TW)
         UAI=1.0/(1.0/(HI*AI)+R)
         TWNEW=(UAI*TX+HO*AO*TS)/(UAI+HO*AO)
C CHECK
         DIFF=ABS(TWNEW-TW)
         IF(DIFF.GT.LIM)THEN
            TW=TWNEW
            GOTO 300
         ENDIF
C END OF LOOP
      RETURN
      END
```

Appendix C

Listing of program CONSTE

Note: subroutines PROP, INSIDE, OUTSIDE, PARAM, and CORREL are identical to the subroutines of the same name in program BENCHMARK, and will not be printed in this appendix.

```
      PROGRAM CONSTE
C
C THIS IS THE SIMPLIFIED VERSION OF TANK WITH A SINGLE UA CAL-
CULATION
C FOR THE ENTIRE TUBE WHICH IS USED TO FIND A CONSTANT EFFEC-
TIVENESS
C WHICH IN TURN IS USED FOR THE SIMULATION IN TIME.
C
      REAL COR(21),TI,TS,LEN,MF,C,OD,ID,EFF,TII(200),MFF(200)
      REAL COEF,NU,K,PR,CP,RHO,DELTIME,TM,QLEN,TX
      REAL DELT,UA,LMTD,HTA,CD,HC,LOSS,MTANK
      INTEGER J,M,D
      CALL CORREL(COR)
C
C INPUT FILES
C
      OPEN(50,FILE='DWBAY.DAT',READ ONLY,STATUS='OLD')
      OPEN(57,FILE='[MATES.ARCHIVE]DWBAY15.ORIG',READ ONLY,
     + STATUS='OLD')
C
C OUTPUT FILES
C
      OPEN(60,FILE='PARAM.DAT',STATUS='NEW')
C      WRITE(60,*)'TIME(MIN)  HXI(C)  TS(C)  Q(W)  UA(W/C)
EFF'
      OPEN(70,FILE='RAYL.DAT',STATUS='NEW')
C
C PARAMETER INPUT
C
      READ(57,*)M,DELTIME
C      WRITE(60,63)M,DELTIME
63    FORMAT(1X,I10,F8.2)
      WRITE(6,*)'M=',M,'DELTIME=',DELTIME
      DO 25,J=1,M
         READ(57,*)TM,D,TII(J),TS,TS,MFF(J),QLEN,UA,TS,TS
         TII(J)=TII(J)+273.15
25    CONTINUE
```

```
      CALL PARAM(TS,LEN,C,OD,ID,COR,HTA,CD,HC)
C
      CALL PROP(TS,COEF,COR,NU,K,PR,CP,RHO)
C
      MTANK=0.409*RHO
C
      LOSS=1.6
C
C THIS LOOP SIMULATES THE TANK-HEAT EXCHANGER OVER TIME,
ADJUSTING THE
C TANK TEMPERATURE EVERY DELTIME MINUTES.
C THE HEAT FLOW PORTION HERE WAS HAND CHECKED GOOD-SPRING BREAK
C
C INITIALIZE TIME: TIME AND HEAT FLOW CALCULATIONS AT ONE TIME
C REPRESENT THE CONDITIONS FOR THE TIME PERIOD FOLLOWING UNTIL
C ANOTHER CALCULATION IS MADE
C
      J=1
      TI=TII(J)
      MF=MFF(J)
C CALCULATE MASS FLOW AT INLET TEMPERATURE
      CALL PROP(TI,COEF,COR,NU,K,PR,CP,RHO)
      MF=MF*(RHO/(60.0*1000.0))
C SIMULATE: CALCULATE THE CONSTANT EFFECTIVENESS
      CALL
SIMULATE(EFF,TI,TS,LEN,MF,OD,ID,COR,QLEN,HTA,CD,HC,C,TM)
C
      TM=0.0
C
      DO 20, J=1,M
C SET MASS FLOW AND INLET TEMPERATURE
         TI=TII(J)
         MF=MFF(J)
C CALCULATE MASS FLOW AT INLET TEMPERATURE
         CALL PROP(TI,COEF,COR,NU,K,PR,CP,RHO)
         MF=MF*(RHO/(60.0*1000.0))
C CHECK FOR ZERO MASS FLOW
         IF(MF.EQ.0.0)THEN
            LMTD=10.0
            TX=TI
            GOTO 40
         ENDIF
C CALCULATE SYSTEM PARAMETERS
         DELT=TI-TS
         TX=TI-EFF*(TI-TS)
         LMTD=(TI-TX)/LOG((TI-TS)/(TX-TS))
40       CONTINUE
         QLEN=MF*CP*(TI-TX)
         UA=QLEN/LMTD
C
```

```
C CONVERT TEMPERATURES AND OUTPUT RESULTS TO FILE
C
         TS=TS-273.15
         TI=TI-273.15
         TX=TX-273.15
         WRITE(60,90)TM,TI,TX,TS,QLEN,UA,EFF
C RETURN TEMPERATURES TO KELVIN
         TS=TS+273.15
         TI=TI+273.15
         TX=TX+273.15
C STEP TIME
         TM=TM+DELTIME
C STEP TANK TEMPERATURE
         CALL PROP(TS,COEF,COR,NU,K,PR,CP,RHO)
         TS=TS+QLEN*DELTIME*60.0/(MTANK*CP)
         TS=TS-LOSS*(TS-293.15)*DELTIME*60.0/(MTANK*CP)
C SET MF BACK TO LITERS/MIN
         CALL PROP(TI,COEF,COR,NU,K,PR,CP,RHO)
         MF=MF/(RHO/(60.0*1000.0))
20     CONTINUE
C
90     FORMAT(1X,F10.1,3F8.2,2F10.2,F8.3)
900    CONTINUE
       STOP
       END
C
C
       SUBROUTINE
SIMULATE(EFF,TI,TS,LEN,MF,OD,ID,COR,QLEN,HTA,CD,HC,C
      +,TM)
C
       REAL EFF,TI,TS,LEN,MF,OD,ID,COR(21),QLEN,HTA,CD,HC,C
       REAL COEF,NU,K,PR,CP,RHO
       REAL PI,TO,HI,TW,DELX,TREF,AI,AO,AC,R,LIM,DIFF
       REAL NUSOUT,HO,RA,NTU,UA,UA1,UA100,TONEW,LOW
       INTEGER I,ITER
C PARAMETER INITIALIZATION
       PI=3.1415927
       LOW=1.0E-04
       DELX=LEN/100.0
       AI=PI*ID*DELX
       AO=HTA*DELX/LEN
       AC=PI*CD*DELX
       IF(AC.EQ.0.0)THEN
          R=0.0
       ELSE
          R=1.0/(HC*AC)
       ENDIF
       QLEN=0.0
       CALL TWALL(TI,TS,TW,OD,COR,DELX,LEN,MF,ID,HTA,CD,HC,C)
```

```
      CALL OUTSIDE(TS,TW,OD,COR,NUSOUT,HO,RA,C)
      CALL INSIDE(TI,HI,MF,ID,COR,TW)
      UA1=1.0/(1.0/(HO*AO)+1.0/(HI*AI)+R)
      UA=100.0*UA1
      TO=TI
      ITER=0
100   CONTINUE
         ITER=ITER+1
         CALL TWALL(TO,TS,TW,OD,COR,DELX,LEN,MF,ID,HTA,CD,HC,C)
         CALL OUTSIDE(TS,TW,OD,COR,NUSOUT,HO,RA,C)
         CALL INSIDE(TO,HI,MF,ID,COR,TW)
         UA100=1.0/(1.0/(HO*AO)+1.0/(HI*AI)+R)
         UA=100.0*((UA1+UA100)/2.0)
         TREF=(TI+TO)/2.0
         CALL PROP(TREF,COEF,COR,NU,K,PR,CP,RHO)
         NTU=UA/(MF*CP)
         EFF=1.0-EXP(-NTU)
         TONEW=TI-EFF*(TI-TS)
         LIM=0.001*(TI-TO)
         IF(LIM.LT.LOW)THEN
            LIM=LOW
         ENDIF
         DIFF=ABS(TONEW-TO)
         IF(DIFF.GT.LIM)THEN
            TO=TONEW
            GOTO 100
         ENDIF
      CONTINUE
      QLEN=MF*CP*(TI-TO)
      RETURN
      END
C
C
      SUBROUTINE
TWALL(TX,TS,TW,OD,COR,DELX,LEN,MF,ID,HTA,CD,HC,C)
C
C THIS SUBROUTINE BALANCES TWO HEAT TRANSFER RATE EQUATIONS IN
ORDER TO
C CALCULATE TW FOR THE BEGINNING AND END OF THE TUBE, AS
SPECIFIED IN
C SUBROUTINE SIMULATE
C           Q = HO*AO*(TW-TS) = UAI*(TX-TW)
C A SUCCESSIVE SUBSTITUTION METHOD IS USED TO ARRIVE AT THE
UNKNOWN
C QUANTITY TW. THE HEAT TRANSFER IS THEN CALCULATED FROM THIS
PARAMETER
C
      REAL TX,TS,TW,OD,COR(21),DELX,LEN,MF,ID
      REAL NUSOUT,HO,HI,DIFF,RA,AI,AO,LIM
      REAL TWNEW,PI,UA,R,UAI,AC
```

```
      REAL COEF,NU,K,PR,CP,RHO,HTA,CD,HC,C
C INITIALIZATION
      PI=3.1415927
      LIM=0.0001
      AI=PI*ID*DELX
      AO=HTA*DELX/LEN
      AC=PI*CD*DELX
      IF(AC.EQ.0.0)THEN
         R=0.0
      ELSE
         R=1.0/(HC*AC)
      ENDIF
C INTIAL GUESS
      TW=(4.0/5.0)*(TX-TS)+TS
C BEGINNING OF SUCCESSIVE SUBSTITUTION LOOP
300   CONTINUE
C LOOP CALCULATES NEW TW
         CALL OUTSIDE(TS,TW,OD,COR,NUSOUT,HO,RA,C)
         CALL INSIDE(TX,HI,MF,ID,COR,TW)
         UAI=1.0/(1.0/(HI*AI)+R)
         TWNEW=(UAI*TX+HO*AO*TS)/(UAI+HO*AO)
C CHECK
         DIFF=ABS(TWNEW-TW)
         IF(DIFF.GT.LIM)THEN
            TW=TWNEW
            GOTO 300
         ENDIF
C END OF LOOP
      RETURN
      END
```

APPENDIX D

Water Property Correlations

The water property correlations were derived from data originating from two sources. The density and coefficient of thermal expansion for water were found using specific volume data for saturated water from Schmidt [9]. The coefficient for thermal expansion, β, was then added to the natural convection property group coefficient for which there is a single correlation. The other water property data was found in the text by Incropera and DeWitt [10]. The correlations were found using the nonlinear curve fitting routine LMDIF1, which is a MINPACK [8] subroutine. Each of the correlations are presented here as a function of temperature T in degrees Kelvin. The correlations are applicable between the temperatures of 280 K and 370 K.

Density kg/m^3

$$\rho = 271.0915 + 6.420254\ T - 0.01772474\ T^2 + 0.1461599E\text{-}04\ T^3$$

Prandtl Number

$$Pr = 0.7408843E\text{-}03 \exp(2642.356/T) + 0.8893757$$

Natural Convection Property Group Coefficient $1/m^3\ K$

$$\frac{\rho^2\ \beta\ C_p\ g}{\mu\ k}\ 10^{-9} = 414.691 - 3.784647\ T + 0.008245761\ T^2$$

Kinematic Viscosity m^2/s

$$\nu\ 10^6 = 0.2324911E\text{-}03\ \exp\ (2407.664/T) + 0.1494501$$

Thermal Conductivity $W/m\ K$

$$k = -0.4890243 + 0.5895468E\text{-}02\ T - 0.7400855E\text{-}05\ T^2$$

Specific Heat $J/kg\ K$

$$C_p = 38938.72 - 415.073\ T + 1.859918\ T^2 - 0.3710142E\text{-}02\ T^3 + 0.2783111E\text{-}05\ T^4$$

Appendix E Hand Calculation of Effectiveness

One method of estimating the performance of an immersed heat exchanger is to calculate a constant effectiveness given a set of flow rate and temperature conditions. The procedure for calculating an effectiveness by hand is presented in this appendix. The method of calculating the effectiveness shown here is the same one that is employed in the constant UA and constant effectiveness programs. An average UA value is calculated for the entire length of the heat exchanger and then the effectiveness is found using the effectiveness NTU relation.

Sample Problem

Hot water flows through an immersed coil which is placed at the bottom of a domestic hot water storage tank. Determine the coil effectiveness given the following coil dimensions and thermal conditions.

Coil Data

Type: Double Wall Bayonet

Length: 5.0 m

Outside Diameter: 16 mm

Inside Diameter: 14 mm

Material: Copper Tube, assume negligible thermal resistance

Natural Convection Enhancement Factor: 1.5

Exterior Heat Transfer Area: 0.9 m^2

Fraction Fin Area: 0.73

Fin Efficiency: 0.8

Contact Radius: 15 mm

Contact Coefficient: 1200 W/m^2 K

Thermal and Hydrodynamic Conditions

Mass Flow: 100 Kg/hr

Heat Exchanger Inlet Temperature: 70 C

Storage Temperature: 20 C

The thermal conditions presented in this problem were the same ones used in the calculation of a constant effectiveness in the yearly simulations done for each of the heat exchangers tested by Farrington. The yearly simulations performed using these effectivenesses compared well with yearly simulations done using variable effectiveness heat exchanger models.

Solution

An average UA will be calculated for the entire tube from an average of the UA calculated at the heat exchanger inlet (UA1) and the UA value at the outlet (UA100). One

hundredth of the length of the tube will be the area used in the calculation of a UA at each end. The average of UA1 and UA100 will be multiplied by 100 to find the overall UA. Water property values will be taken directly from the correlations outlined in appendix D and will be temperature dependent. The hand calculations involve a number of iterations on both the unknown wall temperatures and exit temperatures.

effective exterior heat transfer area calculation (eq. 2.5.1)

$$A_\varepsilon = A_o\ ((1.0-A_f) + A_f\ \eta\ )$$

$$A_\varepsilon = 0.9\ m^2((1.0-0.73) + (0.73)(0.8)) = 0.769\ m^2$$

Inlet UA calculation. UA1 will be calculated for the first one hundredth of the tube area:

$$Dx = 5.0\ m/100\ m = 0.05\ m$$

$$A_\varepsilon = 0.769\ m^2/100.0 = 0.00769\ m^2$$

contact area from eq. 2.5.4

$$A_c = \pi\ CD\ Dx = \pi(0.015\ m)(0.05\ m) = 0.00236\ m^2$$

interior area

$$A_i = \pi\ ID\ Dx = \pi\ (0.014\ m)(0.05\ m) = 0.0022\ m^2$$

wall resistance calculation from eq. 2.5.3

$$R = \frac{1.0}{h_c A_c}$$

$$R = \frac{1.0}{(1200\ W/m^2\ K)(0.00236\ m^2)} = 0.353\ K/W$$

Interior heat transfer coefficient. For the inlet the interior fluid temperature is the inlet temperature

inside cross sectional area

$$A = \pi\ (ID/2.0)^2 = \pi(0.014\ m/2.0)^2 = 1.54E\text{-}04\ m^2$$

mass flow

$$mf = 100\ kg/hr = 0.028\ kg/s$$

density at inlet temperature

$$\rho = 978\ kg/m^3$$

interior velocity

$$U = \frac{mf}{\rho\ A} = \frac{0.028\ kg/s}{(978\ kg/m^3)(1.54E\text{-}04\ m^2)} = 0.186\ m/s$$

inlet kinematic viscosity

$$\nu = 0.4086E\text{-}06\ m^2/s$$

Reynolds number from eq. 2.3.5

$$Re = \frac{U\ ID}{\nu} = \frac{(0.186\ m/s)(0.014\ m)}{0.4086E\text{-}06\ m^2/s} = 6373.0$$

This value of the Reynolds number is in the transition region, so a value for the Nusselt number can be found from a linear interpolation between the laminar and turbulent correlations.

laminar flow (Re=2300) from eq. 2.3.7

$$\overline{Nu}_1 = 3.66$$

turbulent flow (Re=10,000) Nusselt number from Petukhov friction factor from eq. 2.3.2

$$f = (1.82\log(Re) - 1.64)^{-2}$$

$$f = (1.82\log(10,000) - 1.64)^{-2} = 0.0314$$

Prandtl number at the inlet temperature

$$Pr = 2.53$$

Petukhov correlation constants from eq. 2.3.3, 2.3.4

$$K1 = 1.0 + 3.4f = 1.0 + 3.4(0.314) = 1.107$$

$$K2 = 11.7 + 1.8/Pr^{1/3} = 11.7 + 1.8/(2.53)^{1/3} = 13.02$$

The calculation of the wall viscosity depends on a wall temperature, so a value for T_w for the first iteration is assumed to be:

$$T_w = 1/5(T_i - T_s) + T_s$$

$$T_w = 1/5(343.15\ K - 293.15\ K) + 293.15\ K = 303.15\ K$$

dynamic viscosity at wall and bulk temperatures

$$\mu_w = 8.003E\text{-}04\ kg/m\ s$$

$$\mu_b = 3.996E\text{-}04\ kg/m\ s$$

turbulent Nusselt number from eq. 2.3.1

$$\overline{Nu}_t = \frac{(f/8)\ Re\ Pr\ (\mu_b/\mu_w)^{0.25}}{K1 + K2\ (f/8)^{1/2}\ (Pr^{2/3}-1)}$$

$$\overline{Nu}_t = \frac{(0.0314/8)\,(10,000)\,(2.53)\,(3.996/8.003)^{0.25}}{1.107 + 13.02\ (0.0314/8)^{1/2}\ ((2.53)^{2/3}-1)}$$

$$\overline{Nu}_t = 46.22$$

for Re=6373.0 the Nusselt number is

$$\overline{Nu} = \overline{Nu_t} - \frac{(\overline{Nu_t}-\overline{Nu_l})\ (10,000-Re)}{10,000-2300}$$

$$\overline{Nu} = 46.22 - \frac{(46.22-3.66)\,(10,000-6373)}{7700}$$

$$\overline{Nu} = 26.17$$

bulk thermal conductivity

$$k = 0.6625\ W/m\ K$$

heat transfer coefficient from eq. 2.3.6

$$\overline{h_i} = \frac{k\ \overline{Nu}}{ID} = \frac{(0.6625\ W/m\ K)\,(26.17)}{0.014\ m} = 1239\ W/m^2\ K$$

Exterior heat transfer coefficient calculation. Water properties for natural convection are based on the film temperature:

$$T_f = \frac{T_w + T_s}{2.0} = \frac{303.15\ K + 293.15\ K}{2.0} = 298.15\ K$$

Rayleigh number property group from correlation

$$\frac{\rho^2\ \beta\ C_p\ g}{\mu\ k} = 19.3E09\ 1/m^3\ K$$

Rayleigh number from eq. 2.4.2

$$Ra_D = \frac{\rho^2\ \beta\ C_p\ g\ (T_w-T_s)^{0.25}}{\mu\ k}\ OD^3$$

$$Ra_D = (19.3E09\ 1/m^3\ K)\,(0.016m)^3(303.15\ K - 293.15\ K)$$

$$Ra_D = 7.9E05$$

Nusselt number from eq. 2.4.4

$$Nu = M\ C\ Ra_D^{\ m}$$

$$Nu = (1.5)(0.48)(7.9E05)^{0.25} = 21.5$$

film thermal conductivity

$$k = 0.6108\ W/m\ K$$

exterior heat transfer coefficient from eq. 2.4.3

$$h_o = \frac{k\ Nu}{OD} = \frac{(0.6108\ W/m\ K)(21.5)}{0.016\ m} = 820.8\ W/m^2\ K$$

Calculate new wall temperature

UA calculations

$$h_oA_\varepsilon = 820.8\ W/m^2\ K\ (0.00769\ m^2) = 6.31\ W/K$$

$$h_iA_i = 1239.0\ W/m^2\ K\ (0.0022\ m^2) = 2.73\ W/K$$

interior UA from eq. 2.7.4

$$UAI = \frac{1.0}{\frac{1.0}{h_iA_i} + R}$$

$$UAI = \frac{1.0}{\frac{1.0}{2.73\ W/K} + 0.353\ K/W} = 1.39\ W/K$$

the new wall temperature is then found from eq. 2.9.3

$$T_{wnew} = \frac{UAI\ T_i + h_oA_\varepsilon\ T_s}{UAI + h_oA_\varepsilon}$$

$$T_{wnew} = \frac{(1.39\ W/K)(343.15\ K) + (6.31\ W/K)(293.15\ K)}{1.39W/K + 6.31W/K}$$

$$T_{wnew} = 302.18\ K$$

The new value for the wall temperature can then be used to recalculate the UA at the inlet, an iteration procedure which ends when the wall temperature changes less than 0.0001 K. The final thermal variables for the inlet section in this example problem are listed below:

T_{wall} = 302.22 K

h_i = 1183.63 W/m^2 K

h_o = 793.39 W/m^2 K

UA1 = 1.106 W/K

Heat Exchanger Exit

The initial calculation of the exit UA, or UA100, must be based on an assumed exit temperature. The heat exchanger inlet temperature is selected as the first guess, which in this case is 343.15 K. The wall temperature for the final section is calculated using the same method that was employed for the inlet UA1. The value of UA100 in the first iteration is then equal to the value of UA1:

UA100 = 1.106 W/K

A new estimate for the exit temperature is then found using the effectiveness NTU relationship.

the UA for the tube is found:

$$UA = 100 \frac{UA1 + UA100}{2.0}$$

which, for the first iteration, is:

$$UA = 110.6 \text{ W/K}$$

the number of thermal units is then found from eq. 2.9.4

$$NTU = \frac{UA}{mf\ C_p}$$

The specific heat is found at the arithmetic average of the inlet and exit temperatures, which for the first iteration is the inlet temperature or 343.15 K.

$$C_p = 4190.5 \text{ J/kg K}$$

the value of NTU is then

$$NTU = \frac{110.6 \text{ W/K}}{(0.028 \text{ kg/s})(4190.5 \text{ J/kg K})} = 0.943$$

the effectiveness is then found from eq. 2.9.5

$$\varepsilon = 1.0 - e^{-NTU} = 1.0 - e^{-0.943} = 0.61$$

a new value for the exit temperature can be found:

$$T_{onew} = T_i - \varepsilon\ (T_i - T_s)$$

$$T_{onew} = 343.15 \text{ K} - 0.61(343.15 \text{ K} - 293.15 \text{ K})$$

$$T_{onew} = 312.6 \text{ K}$$

The new exit temperature can then be used to calculate a new value for UA100, which in turn is used to find a new UA value for the entire tube and a new exit temperature. This iteration procedure may be carried out until the new exit temperature changes less than one thousandth of the difference between the

inlet and storage tank temperatures. The values of the thermal variables at the exit section after this iteration are:

$$h_i 100 = 716.35 \text{ W/m}^2 \text{ K}$$

$$h_o 100 = 607.62 \text{ W/m}^2 \text{ K}$$

$$UA100 = 0.83 \text{ W/K}$$

the overall UA is then

$$UA = 100 \frac{1.106 \text{ W/K} + 0.83 \text{ W/K}}{2.0} = 96.82 \text{ W/K}$$

the final effectiveness is also a result of the iteration

$$\varepsilon = 0.5734$$

and the exit temperature is

$$T_o = 314.5 \text{ K}$$

The effectiveness calculated here for the proposed heat exchanger can be compared with the effectiveness of other designs performing under similar thermal conditions. Simulations may also be run using the constant effectiveness calculated here to estimate yearly performance for a system with this heat exchanger.

References

1. Duffie, J.A., and Beckman, W.A., Solar Engineering of Thermal Processes, Wiley Interscience, New York, 1980, Chapter 10.2.

2. University of Wisconsin Solar Energy Laboratory, "TRNSYS, a Transient Simulation Program," Engineering Experiment Station Report 38-11, Madison, (1981).

3. Mitchell, J.C., et al., "FCHART 4.1--A Design Program for Solar Heating Systems," University of Wisconsin-Madison, Engineering Experiment Station Report 50, (1982).

4. Feiereisen, T., "An Experimental Study of Immersed Coil Heat Exchangers," Master's thesis, Madison, WI: University of Wisconsin, 1982.

4a. Feiereisen, T., Klein, S.A., Duffie, J.A., and Beckman, W.A.,"Heat Transfer from Immersed Coils," ASME 82-WA/Sol-18, Madison, WI: University of Wisconsin, 1982.

5. Farrington, R.B., and Bingham, C.E., Testing and Analysis of Immersed Heat Exchangers, SERI/TR-253-2866, Golden, CO: Solar Energy Research Institute, Aug. 1986.

6. Petukhov, B.S., "Heat Transfer and Friction in Turbulent Pipe Flow with Variable Physical Properties," Advances in Heat Transfer, Vol. 6, Academic Press, New York, 1970, p. 503.

7. Morgan, V.T., "The Overall Convective Heat Transfer from Smooth Circular Cylinders," Advances in Heat Transfer, Vol. 11, Academic Press, New York, 1975, pp. 199-264.

8. Minpack Routines, Argonne National Laboratory, February 1980.

9. Schmidt, E., Properties of Water and Steam, SI Units, Technische Universitat, Munchen, 1979, pp. 22.

10. Incropera, F.P., and DeWitt, D.P., Fundamentals of Heat Transfer, John Wiley & Sons, New York, 1981, pp. 782-783.

10a. Incropera, F.P., and DeWitt, D.P., Fundamentals of Heat Transfer, John Wiley & Sons, New York, 1981, pp. 112-117.

11. Ozisik, M.N., Heat Transfer, McGraw-Hill, New York, 1985, pp. 281-339.

12. Box, G.E.P., Hunter, W.G., and Hunter, J.S., Statistics for Experimenters, John Wiley & Sons, New York, 1978, pp. 453-509.

13. Marsters, G.F., "Arrays of Heated Horizontal Cylinders in Natural Convection," International Journal of Heat and Mass Transfer, Vol. 15, 1972, pp. 921-933.

14. Sparrow, E.M., and Niethammer, J.E., "Effect of Vertical Separation Distance and Cylinder-to-Cylinder Temperature Imbalance on Natural Convection for a Pair of Horizontal Cylinders," ASME Journal of Heat Transfer, Vol. 103, November 1981, pp. 638-644.

15. Sparrow, E.M., and Boessneck, D.S., "Effect of Transverse Misalignment on Natural Convection From a Pair of Parallel, Vertically Stacked, Horizontal Cylinders," ASME Journal of Heat Transfer, Vol. 105, May 1983, pp. 241-247.

16. Sparrow, E.M., and Pfeil, D.R., "Enhancement of Natural Convection Heat Transfer From a Horizontal Cylinder due to Vertical Shrouding Surfaces," ASME Journal of Heat Transfer, Vol. 106, February 1984, pp. 124-130.